A Section 508–conformant HTML version of this article is available at https://doi.org/10.1289/EHP15503.

Perinatal Exposure to Lead or Diethylhexyl Phthalate in Mice: Sex-Specific Effects on Cardiac DNA Methylation and Gene Expression across Time

Kai Wang,[1] *Minghua Li,*[1] *Maureen A. Sartor,*[1,2] *Justin A. Colacino,*[3,4] *Dana C. Dolinoy,*[3,4] *and Laurie K. Svoboda*[3,5]

[1]Department of Computational Medicine and Bioinformatics, Medical School, University of Michigan, Ann Arbor, Michigan, USA
[2]Department of Biostatistics, School of Public Health, University of Michigan, Ann Arbor, Michigan, USA
[3]Department of Environmental Health Sciences, School of Public Health, University of Michigan, Ann Arbor, Michigan, USA
[4]Department of Nutritional Sciences, School of Public Health, University of Michigan, Ann Arbor, Michigan, USA
[5]Department of Pharmacology, Medical School, University of Michigan, Ann Arbor, Michigan, USA

Background: Global and site-specific changes in DNA methylation and gene expression are associated with cardiovascular development, aging, and disease, but how the transcriptome and epigenome of the heart change across the life course in males vs. females and how chemical exposures early in life influence this programming have not yet been investigated.

Objectives: We used an established mouse model of developmental exposures to investigate the effects of perinatal exposure to either lead (Pb) or diethylhexyl phthalate (DEHP), two ubiquitous environmental contaminants that are both strongly associated with cardiovascular diseases (CVDs), on DNA methylation and gene expression across the life course in whole hearts.

Methods: Dams were randomly assigned to receive human physiologically relevant levels of Pb (32 ppm in water), DEHP (25 mg/kg chow), or control water and chow. Exposures started 2 weeks prior to mating and continued until weaning at postnatal day 21 (3 wk of age). Approximately 1 male and 1 female offspring per litter were followed to 3 wk, 5 months, or 10 months of age, at which time whole hearts were collected ($n \geq 5$ per sex per exposure). Enhanced reduced representation bisulfite sequencing (ERRBS) was used to assess the cardiac DNA methylome at 3 wk and 10 months, and RNA-Seq was conducted at all three time points. MethylSig and edgeR were used to identify age-related differentially methylated regions (DMRs) and differentially expressed genes (DEGs), respectively, within each sex and exposure group. Cell type deconvolution of bulk RNA-Seq data was conducted using the MuSiC algorithm and publicly available single-cell RNA-Seq data.

Results: Thousands of DMRs and hundreds of DEGs were identified in control, DEHP, and Pb-exposed hearts across time between 3 wk and 10 months of age. A closer look at the genes and pathways showing differential DNA methylation revealed that the majority were unique to each sex and exposure group. Overall, pathways governing development and differentiation changed across time in all conditions. A small number of genes in each group showed significant differences in DNA methylation and gene expression with life stage, including several that were different in toxicant-exposed but not control mice. We also observed subtle but significant differences in the proportion of several cell types that were associated with life stage, sex, or developmental exposure.

Discussion: Together these data suggest that gene expression and DNA methylation programs, as well as cellular composition, may differ across the life course long after cessation of exposure in perinatal Pb- or DEHP-exposed mice compared to controls and highlight potential biomarkers of developmental toxicant exposures; however, additional studies are required for confirmation. Further studies are also needed to investigate how epigenetic and transcriptional differences impact cardiovascular health across the life course, particularly in old age when the risk of cardiovascular diseases is markedly increased. https://doi.org/10.1289/EHP15503

Introduction

Cardiovascular diseases (CVDs) comprise an array of conditions, including atherosclerosis, heart failure, myocardial infarction, hypertension, cardiac arrhythmias, congenital heart defects, and stroke.[1,2] In spite of advancements in prevention, diagnosis, and treatment, CVDs remain a leading cause of death in the United States and around the world.[3,4] CVD risk and pathogenesis are strongly influenced by several factors, including sex, age, diet, lifestyle, and environmental exposures.[5–8] Among these variables, age is the strongest risk factor.[9] Aging is reflected in both the passage of time since birth (chronological aging), as well as the declines in physiological processes that occur over time (biological aging).[10] Genetic, environmental, and lifestyle factors may influence the rate of biological aging, resulting in a biological age that is higher or lower than one's chronological age.[10–12] Notably, several factors that accelerate biological aging are associated with CVDs, including genetic progeroid syndromes, diet, exercise, cigarette smoking, psychosocial stress, and cancer treatments.[10,13–15] Aging in the cardiovascular system is characterized by widespread changes in the epigenome, including alterations in DNA methylation and chromatin organization.[16] Recent work demonstrates that DNA methylation signatures of accelerated aging are associated with diminished cardiovascular health and increased CVD.[17,18] However, despite this evidence, it is unclear how exposure to common environmental pollutants during critical windows of development influence epigenetic programming and gene expression across the life course in the heart. Moreover, although CVDs exhibit marked sexual dimorphism,[5,6,19] potential sex differences in epigenetic regulation of gene expression across the lifespan are poorly understood.

The metal lead (Pb) and the plasticizer di(2-ethylhexyl)phthalate (DEHP) are chemically distinct environmental pollutants that differ greatly in their toxicokinetics and toxicodynamics.[20,21] Nevertheless, both chemicals are strongly associated with various CVDs. In the United States, sources of human exposure to Pb include legacy drinking water systems, contaminated household dust and soil, imported food and consumer products, aviation fuel, and industrial processes.[22,23] In spite of numerous initiatives to ban

Address correspondence to Laurie K. Svoboda, M6232 SPH II, 1415 Washington Heights, Ann Arbor, MI 48109-2029 USA. Email: lmyrant@umich.edu

Supplemental Material is available online (https://doi.org/10.1289/EHP15503).

The authors declare no conflicts of interest.

Conclusions and opinions are those of the individual authors and do not necessarily reflect the policies or views of EHP Publishing or the National Institute of Environmental Health Sciences.

Received 3 June 2024; Revised 15 April 2025; Accepted 1 May 2025; Published 16 June 2025.

Note to readers with disabilities: *EHP* strives to ensure that all journal content is accessible to all readers. However, some figures and Supplemental Material published in *EHP* articles may not conform to 508 standards due to the complexity of the information being presented. If you need assistance accessing journal content, please contact ehpsubmissions@niehs.nih.gov. Our staff will work with you to assess and meet your accessibility needs within 3 working days.

the use of Pb in paints, gasoline, and other consumer products worldwide, Pb exposure remains a significant public health threat. DEHP is a plasticizer widely used in building materials, plumbing, toys, food packaging, pharmaceuticals, and medical tubing.[24] Although the US government and some states have set guidelines regulating DEHP levels in air, water, and consumer products, human exposure to this chemical is still widespread.[25] Both Pb and DEHP exposures are associated with numerous adverse cardiovascular outcomes in human population studies, including congenital heart defects, heart failure, hypertension, cardiac arrhythmias, myocardial infarction, and stroke in Pb exposed individuals[26–30] and hypertension, atherosclerosis, coronary artery disease, decreased heart rate variability, and increased all-cause CVD mortality in individuals exposed to DEHP and its metabolites.[31–36] Not surprisingly, co-exposures to both toxicants have been reported in human population studies,[37,38] and *in vitro* and animal toxicology studies suggest that the exposures may have synergistic effects.[39,40]

Offspring can be exposed to both Pb and DEHP via placental transfer as well as in breast milk.[41–44] Developmental exposures to both Pb and DEHP have been shown to impact the epigenome in noncardiac tissues in human[45,46] and animal studies,[47–50] and we recently demonstrated that perinatal exposure to these chemicals also impacts sex-specific DNA methylation in the heart in adolescence and early adulthood in mice.[51,52] However, the effects of environmental contaminant exposures during early development on epigenetic regulation of gene expression across the life course, and potential differences by sex, have not been investigated to our knowledge. To address this knowledge gap, in this study, we build upon our previous work by examining the effects of exposure to Pb and DEHP during gestation and lactation on normal DNA methylation and gene expression across time in the heart in both male and female mice, in puberty/adolescence, young adulthood, and middle adulthood.

Materials and Methods

Mice and Exposure Paradigm

The work outlined here was part of a larger developmental exposure study conducted by the National Institute of Environmental Health Sciences (NIEHS) Toxicant Exposures and Responses by Genomic and Epigenomic Regulators of Transcription (TaRGET II) Consortium, which sought to determine how developmental environmental exposures impact the epigenome in multiple tissues and time points across the life course.[53] Mouse Pb and DEHP exposures were performed as outlined previously.[52,54] Mice utilized for these experiments were wild-type a/a nonagouti mice derived from a colony of the viable yellow agouti (A^{vy}) strain maintained in the male line for more than 230 generations (colony maintained in-house at the University of Michigan). This results in forced heterozygosity on an invariant genetic background and mice that are 93% identical to the C57BL/6J strain.[55,56] The exposure period began in periconception (2 wk prior to mating), continued through gestation and lactation, and stopped at weaning at 3 wk of age. Two weeks prior to mating with virgin a/a males, 8- to 10-wk-old virgin females were randomly assigned to control, DEHP (via chow), or Pb (via drinking water) exposure groups. DEHP (Sigma, catalog number 07-3083, 98% purity) was dissolved in 7% corn oil and administered via chow (25 mg per kg chow). Mixing of DEHP into the chow (AIN-93G, TD95092, Harlan Teklad) was carried out by the manufacturer. This results in an estimated maternal DEHP dose of 5 mg/kg/day, assuming that pregnant and lactating female mice weigh ∼25 g and eat 5 g of chow per day.[57] The doses used here have been used in other rodent studies, resulting in an amniotic fluid DEHP level of 68 ng/mL.[58] This is comparable to the range of levels reported in human studies of DEHP in amniotic fluid (1.6 to 22.1 ng/mL, and a maximum level of 100 ng/mL).[59–63] Likewise, it is within or below the range of no observed adverse effect levels (NOAELs) reported by US and European agencies, between 3 and 23 mg/kg/day.[64,65] Pb II acetate trihydrate (Sigma Aldrich, >99% purity) was dissolved in distilled water to create a 50 mM stock solution, which was then diluted into drinking water at a concentration of 32 ppm. This resulted in a blood lead level of 16–60 μg/dL in the pregnant dams, based on our previously published study.[66] This blood Pb level is comparable to historical human exposures in the US (5 to >30 μg/dL)[67] and current Pb exposures worldwide (∼4 to 45 μg/dL reported in Chinese and Mexican cohorts).[68,69] Pb concentrations in water were verified using inductively coupled plasma mass spectrometry (ICPMS) with a limit of detection of 1.0 μg/L (conducted at NSF International). Exposures were stopped at weaning, and mice from all exposure groups were administered standard chow and drinking water for the duration of the study. Mice were housed with three to four animals per cage. There were five to seven mice in each experimental group. Seven mating pairs per exposure group were utilized for the study, for a total of 21 mating pairs. All matings resulted in pregnancies, with the exception of one DEHP-exposed dam, which was injured by the male mate. The exposure paradigm and sample sizes are outlined in Figure 1.

Animal Monitoring, Euthanasia, and Tissue Collection

Animals were monitored daily for signs of illness or distress and were weighed weekly. Approximately one male and one female offspring per litter was sacrificed at three time points: at weaning on postnatal day 21, at 5 months of age, and at 10 months of age. These time points represent infancy, early adulthood, and middle age, respectively, in humans.[70] Thus, this period spans early childhood and the pubertal transition and extends through midlife. Animals were sacrificed via CO_2 asphyxiation and bilateral pneumothorax per protocols approved by the University of Michigan Institutional Animal Care and Use Committee.[71] At sacrifice, a final weight measurement was collected, and mice were euthanized according to protocols established by the NIEHS TaRGET II Consortium.[71] Hearts were extracted, weighed, snap frozen in liquid nitrogen, and stored at −80°C until further processing. RNA and DNA were extracted using the AllPrep kit (Qiagen) according to manufacturer instructions.

Enhanced Reduced Representation Bisulfite Sequencing

Enhanced reduced representation bisulfite sequencing was performed at the University of Michigan Epigenomics Core as outlined previously.[72] Unless otherwise specified, all enzymes and reagents were purchased from New England Biolabs (NEB). Fifty nanograms of genomic DNA was utilized for each sample (to which 0.5% unmethylated lambda DNA was added as bisulfite conversion control spike-in), digested overnight with MspI, purified using phenol:chloroform extraction, and resuspended in 10 mM Tris pH 8.0. The digested DNA was prepared for adapter ligation in two steps each followed by cleanup using Qiagen Qiaquick PCR purification kit. The DNA fragments were first repaired and phosphorylated using T4 DNA polymerase, Klenow DNA polymerase, and T4 polynucleotide kinase. The second stop involved addition of a single adenine nucleotide to the 3′ end of the fragments using Klenow fragment enzyme. Ligation of methylated stubby adapters was done with the T4 DNA ligase during an overnight incubation at 16°C. The adapter ligated fragments were cleaned using two rounds cleanup using AMPure XP magnetic beads. The first elution was done in 50 μL of 10 mM Tris pH 8.0, while the second was done in 20 μL of the same buffer. Size selection was done on a 1.8% agarose (BioRad catalog number 161-3106)-ethdium bromide gel run at 65 V for 115 min to separately enrich fragments in the range of 100–200 bp and 200–400 bp. Each enriched fragment was separately processed in

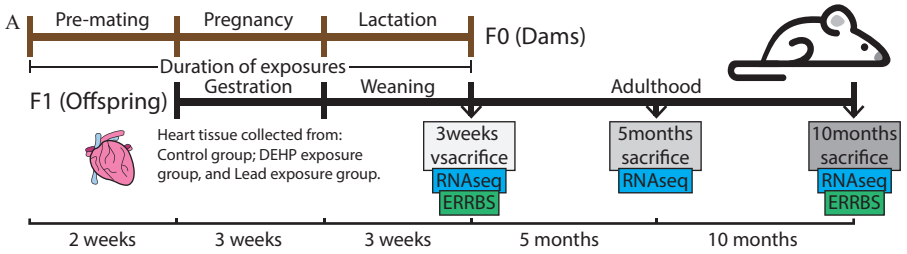

B Number of Animals (ERRBS)

	3 weeks		10 months	
	M	F	M	F
Ctrl	7	7	6	6
DEHP	6	5	6	6
Lead	7	7	5	5

C Number of Animals (RNA-seq)

	3 weeks		5 months		10 months	
	M	F	M	F	M	F
Ctrl	6	6	6	6	6	6
DEHP	6	6	7	5	6	6
Lead	6	7	6	6	6	5

Figure 1. (A) Diagram depicting the exposure paradigm and overall experimental design. Dams were exposed to control, DEHP, or Pb beginning 2 wk prior to mating, and exposure continued through gestation and lactation. Exposures ceased at weaning, and separate cohorts of male and female mice were sacrificed at three time points: weaning, 5 months of age, and 10 months of age. ERRBS was conducted in hearts from offspring at 3 wk and 10 months of age, and RNA-seq was conducted in hearts from all thee time points. (B, C) Number of animals in each sex/exposure group. Note: Ctrl, control; DEHP, diethylhexyl phthalate; ERRBS, enhanced reduced representation bisulfite sequencing; F, female; M, male; Pb, lead.

the following steps. Purification from agarose was done using the Qiagen QIAquick Gel extraction kit according to the manufacturer's protocol. The DNA fragments were treated with the Zymo EZ DNA methylation kit (Zymo Research) using the following PCR incubation program: 55 cycles of 95°C for 30 s and 50°C for 15 min followed by an incubation at 4°C for 10 min to 1 h. Bisulfite-converted DNA was cleaned according to the manufacturer's instructions, and products were dual indexed by PCR using NEB Dual Index Primer Pair primers in the presence of HiFi Polymerase (Roche) for a total of 18 cycles. The final libraries were cleaned up with AMPure XP beads (product number A63880, Beckman Coulter). DNA quantity was measured using the Qubit (ThermoFisher), and library size was assessed using the 2200 TapeStation High Sensitivity D1000 kit (Agilent Technologies). Sequencing was conducted at the UM Advanced Genomics Core on the Illumina NovaSeq 6000 using an S1 100-cycle flow cell, with an average sequencing depth of ~49 M. Bisulfite conversion efficiencies (calculated from unmethylated Lambda spike-in) for all samples were at least 98.4% (average 99.3%), and the average mapping efficiency was 65.3%. Quality control (QC) criteria are outlined in Excel Table S1. On average, this method captured 5% of genomic CpGs.

RNA-Seq

RNA processing, library preparation, and sequencing were carried out at the University of Michigan Advanced Genomics Core. RNA quantity and quality were first verified using Qubit and Agilent 2200 TapeStation, respectively. Library preparation was conducted using the KAPA mRNA Hyper Prep Kit (Roche) with dual indexing adapters. Library quality was verified using the Agilent 2200 TapeStation. Sequencing was performed using the Illumina NovaSeq 6000 using an S2 flow cell and paired end, 50 bp reads. Average sequencing depth was ~60 M.

Quality Control of ERRBS and RNA-Seq Data

For quality control of enhanced reduced representation bisulfite sequencing (ERRBS) and RNA-Seq data, FastQC (version 0.11.8; Babraham Bioinformatics) was used to assess the overall quality of each sequenced sample. TrimGalore (version 0.4.5; Babraham Bioinformatics) was applied to remove adaptor sequences and trim low-quality bases. After trimming, reads with a length < 20 nucleotides were removed from further analysis for both ERRBS and RNA-Seq. Bismark (version 0.22.1) with Bowtie2 (version 2.3.4)[73,74] as backend was used for reads alignment and methylation calling for the ERRBS data with default settings (multiseed length of 20 bp with 0 mismatches). The unmethylated lambda phage DNA was used to calculate the bisulfite conversion rates. STAR (version 2.7.1a)[75] was used to perform reads alignment for RNA-Seq data. HtSeq-count (version 0.11.2)[76,77] with Python (version 3.7.3; python.org) was applied to generate the final reads count. Genome Reference Consortium Mouse Build 38 (mm10) was used as the reference genome for both ERRBS and RNA-Seq data.

DEG and DMR Analysis

The Bioconductor packages RUVSeq (version 1.32.0)[77] and edgeR (version 3.40.2)[78] were used to correct the batch effects and identify the differentially expressed genes, respectively. The *RUVr* function with $k = 3$ was applied to remove any potential batch effects among the three time points of the RNA-Seq data within each treatment group. Genes with at least five reads counted in at least 12 animals were kept for further differentially expressed gene (DEG) analysis. To identify DEGs across time, three comparisons, i.e., PND21 vs. 5 month, 5 month vs. 10 month, and PND21 vs. 10 month, were performed within each treatment group. Male data and female data were analyzed separately. Significant DEGs were defined for all comparisons, as those genes with false discovery rate (FDR) < 0.05 and absolute log fold change > 2. In addition, using limma (version 3.54.2),[79] we ran a combined model with two different interaction terms separately: ~sex + age + exposure + W1 + W2 + W3 + endothelial + smooth muscle cells + ventricular cardiomyocyte + age × exposure and ~sex + age + exposure + W1 + W2 + W3 + endothelial + smooth muscle cells + ventricular cardiomyocyte + age × sex (W1, W2, and W3 are covariates for batch correction). This analysis aimed to identify genes that were significantly different between life stages, regardless of sex or exposure. The same significance cutoffs were applied to identify DEGs using the combined model. Comparative Toxicogenomics Database[80] (release 17204) was used to examine the chemical interactions of certain DEGs.

The Bioconductor package methylSig (version 0.5.2)[81] was used to identify differentially methylated regions. A tiling window with 100 nucleotides was applied for differentially methylated region (DMR) detection. CpG sites with < 10 and more than 500 reads covered were removed from further analysis. Tiling windows with required coverage in at least four samples per comparison group were used for DMR detection. DMRs were identified using the *methylSigDSS* function between PND21 and 10 months within

each treatment group and sex. An FDR < 0.05 and methylation change larger than 10% were used to select significant DMRs. The Bioconductor package annotatr (version 1.24.0)[82] was used to annotate the DMRs to different genomic regions, including CpG islands, CpG shores, CpG shelves, CpG intervals, promoters, exons, introns, 5′ untranslated regions (UTRs), 3′UTRs, enhancers, and 1–5 kb upstream of transcription start sites (TSSs), and criteria for each annotation are described in the supplemental material for reference.[82] The genomic annotations are originally from the AnnotationHub R package.[83] Furthermore, we combined ERRBS data from all samples and ran a combined model with two different interaction terms separately (~age + exposure + sex + age × exposure and ~age + exposure + sex + age × sex) with limma (version 3.54.2)[79] to identify any genomic regions that were significantly enriched between 3 wk and 10 months, regardless of sex or exposure. The same significance cutoffs were applied to identify DMRs using the combined model.

Gene Ontology analysis of DEGs and DMRs. The Bioconductor packages clusterProfiler (version 4.6.2)[84] and ChipEnrich (version 2.22.0)[85] were used to perform Gene Ontology (GO) analysis with DEGs and DMRs, respectively. The *enrichGO* function in clusterProfiler with DEGs as input was used to identify related GO terms. For DMRs, the *chipenrich* function with locus definition *nearest_tss* (the region spanning the midpoints between the TSSs of adjacent genes) was applied to discover enriched GO terms. All three ontologies, biological process (BP), cellular component (CC), and molecular function (MF), were used in both DEG- and DMR-related GO analysis. An FDR < 0.05 cutoff was used to select significantly enriched GO terms.

Cell Type Deconvolution of Bulk RNA-Seq Data

To quantify whether transcriptional differences with exposure or aging were associated with alterations in cell type composition of heart tissues, we used a bioinformatic deconvolution method based on a single-cell atlas of the normal heart, based on data generated as part of the Human Cell Atlas.[86] Sample-specific counts matrices of single-cell RNA-Seq profiling of hearts were downloaded from the Human Cell Atlas Data Explorer and loaded into Seurat (version 4.3.0).[87] These data were downsampled to 25,000 cells via the "subset" function, and we then used these single-cell gene expression data to predict the cellular composition of our tissues based on their bulk RNA-Seq profiles. For this deconvolution, we used the multi-subject single-cell (MuSiC) deconvolution method (version 1.0.0),[88] which predicts cell type proportions in bulk RNA-Seq data based on a reference multisubject single-cell RNA-Seq dataset. Mouse-to-human gene alignment occurred with BioMart,[89] and then MuSiC uses a nonnegative least squares regression-based method based on the cell type–specific gene expression signatures from the single-cell data, with constraints that individual cell type proportions must be a positive value and their sum cannot exceed 1. The cell proportion differences over time or exposure were tested for statistical significance by one-way analysis of variance (ANOVA).

Results

Effects of Pb and DEHP Exposure on Heart Weights

Mice were exposed to Pb or DEHP beginning 2 wk prior to mating through weaning. Pups were evaluated at 3 wk, 5 months, or 10 months. No significant differences in heart weight of mice exposed perinatally to Pb to that of control mice were observed at either 3 wk or 5 months of age.[51,54] In this study, we evaluated this end point in additional cohorts of mice: 3-wk-old mice exposed to DEHP and 10-month-old mice exposed to either Pb or DEHP. No significant differences in heart weight to body weight ratio were observed for any condition (Figure S1).

Table 1. Number of significantly differentially methylated regions (DMRs) between 3 weeks and 10 months.

	Male		Female	
Exposure	Hypo	Hyper	Hypo	Hyper
Control	797	2,879	720	2,935
DEHP	647	2,849	329	1,697
Pb	769	3,336	530	2,817

Note: Significance was based on an FDR < 0.05 and absolute methylation difference >10%. $n = 5$–7 mice per condition, as outlined in Figure 1. DEHP, diethylhexyl phthalate; Pb, lead.

DNA Methylation Differences between PND21 and 10 Months of Age in Mice Perinatally Exposed to Control, Pb, or DEHP

To examine how Pb and DEHP exposure affected DNA methylation during the period from early development and into adulthood, we conducted ERRBS in whole hearts at weaning and 10 months of age, with each treatment group having 5–7 animals per sex (Figure 1B). We determined the number of differentially methylated regions (i.e., between weaning and 10 months of age) in each treatment group, which is summarized in Table 1 and Figure S2. In each group, we observed several thousand DMRs, with the majority (78%–84%) being hypermethylated (Table 1). In both sexes, mice exposed to either Pb or DEHP demonstrated slightly greater percentage of DMRs showing hypermethylation compared to control (Table 1). We next annotated the DMRs in each condition to the mouse mm10 genome and found that enrichment of DMRs between the two time points differed based on the direction of methylation change. Compared to all genomic regions tested, hypomethylated DMRs were less likely to be found in CpG islands, shelves, exons, introns, 3′UTRs, and enhancers. In contrast, hypermethylated DMRs were slightly enriched for several of these regions, including CpG islands, exons, introns, and enhancers (Figure 2). These patterns were qualitatively similar across sex and exposure group. Lists of annotated, age-related DMRs for each sex and exposure group are included in Excel Table S2. To increase statistical power and identify life stage DMRs that were present across all conditions, we utilized a combined model including all samples from two time points, both sexes, and all exposure groups. Using this model with the interaction term of age × exposure, we found 1,612 significantly enriched DMRs corresponding to life stage; 1,385 (86%) of these DMRs were also detected in the sex- and exposure-specific analysis. With the interaction term of age × sex, there were 1,848 significantly enriched DMRs corresponding to life stage; 1,535 (83%) of these DMRs were also detected in the sex- and exposure-specific analysis (Excel Table S3).

Pathways Undergoing Differential Methylation between PND21 and 10 Months of Age in Mice Perinatally Exposed to Control, Pb, or DEHP

In order to understand the biological pathways undergoing differential DNA methylation, we conducted pathway analysis using ChIPEnrich, stratifying by sex, exposure, and direction of methylation change. The results of this analysis are shown in Figure 3 and in Excel Table S4. Figure 3A summarizes significant Gene Ontology biological process (GOBP) terms for each combination of sex, exposure, and direction of methylation change, which are relevant to cardiovascular development and disease. An upset plot depicting overlaps among all of the enriched GO terms (GOBP, GOCC: Gene Ontology Cellular Component, GOMF: Gene Ontology Molecular Function) is shown in Figure S3 and demonstrates that the majority

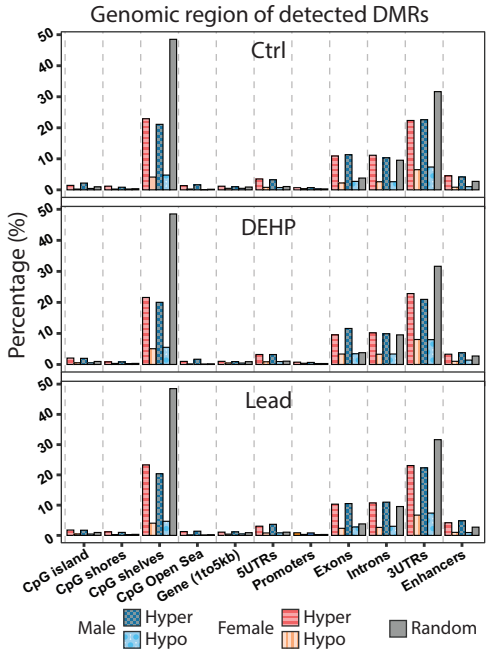

Figure 2. Genomic regions of significantly enriched DMRs comparing 3 wk to 10 months of age within each exposure group. Percentage of DMRs mapping to the mouse reference genome (mm10) compared to what would be expected in a random distribution, stratified by sex and direction of methylation change. Hyper indicates higher DNA methylation levels in 10-month samples compared to 3-wk samples, while hypo means higher DNA methylation levels in 3-wk samples compared to 10-month samples. Data for this figure can be found in Table S2, and genomic regions were defined using the Bioconductor package anatotr. $n = 5$–7 mice per condition, as outlined in Figure 1. Note: Ctrl, control; DEHP, diethylhexyl phthalate; DMR, differentially methylated region; UTR, untranslated region.

of enriched GO terms fall within a single condition. Overall, differential DNA methylation occurred in pathways associated with differentiation, disease, and development (Figure 3A; Excel Table S4). A closer examination of the significant pathways specifically related to cardiovascular development and disease showed that the majority of enriched pathways occurred within a single sex/exposure combination, although pathways related to embryonic development, pattern specification, response to vascular endothelial growth factor stimulus, animal organ regeneration, and cardiac hypertrophy were enriched in multiple conditions (Figure 3A). Enriched pathways also differed based on the direction of DNA methylation change, underscoring the importance of stratifying on the basis of hyper vs. hypomethylated DMRs. Notably, a few pathways were enriched in exposed animals but not in control or *vice versa*. For example, the hypomethylated DMRs in DEHP-exposed males and females were enriched for cardiac muscle hypertrophy, while hypo and hypermethylated control females, but not exposed animals, showed enrichment for animal organ regeneration (Figure 3A). Figure 3B–E illustrates the total number of significantly enriched GOBP pathways for each condition. The numerator of each fraction represents the number of pathways containing heart-specific terms (muscle, ventricular, atrial, cardiac, aorta, and heart) and the denominator all other pathways, and the data show that the number of total and heart-specific pathways differed across exposure groups.

Temporal Gene Expression Differences in Mice Perinatally Exposed to Control, Pb, or DEHP

We next examined how the cardiac transcriptome differed across the life course in males vs. females and the effects of chemical exposures on this process. To this end, we conducted RNA-Seq on samples of RNA from the same hearts utilized for ERRBS (5–7 animals per condition) (Figure 1C) at weaning and 10 months of age, as well as an additional cohort of animals at 5 months of age. Volcano plots depict the number, magnitude, and direction of differences in gene expression for each sex and exposure, comparing weaning and 10 months of age (Figure S4A–F). Volcano plots depicting comparisons between weaning vs. 5 months of age and 5 months vs. 10 months of age are shown in Figure S4G–R. Numbers of differentially expressed genes (DEGs) are also summarized in Table 2, and the full lists of DEGs can be found in Excel Tables S5–S7. We found several hundred DEGs between weaning and 10 months of age in all exposures/sexes, with the largest number of DEGs (933) occurring in control female hearts (Table 2). Within each exposure group, the majority of differences in gene expression between time points were sex specific; however, there were several genes in common across sexes (Figure 4A). When we compared gene expression differences across exposure groups, we found that the majority of differentially expressed genes were unique to each exposure (Figure 4B). To identify DEGs associated with life stage across all conditions, we again performed a combined model including samples from all three time points, both sexes, and all three exposure groups, which revealed fewer DEGs. With the interaction term of age × exposure, only 70 and 141 DEGs were identified for the comparisons of 3 wk vs. 5 months and 3 wk vs. 10 months, respectively (Excel Table S8). Sixty-eight (97%) of 70 DEGs from the 3 wk vs. 5 month comparison were also identified in the sex- and exposure-specific analysis, while 133 (94%) of the 141 DEGs from the combined model were also identified in the sex- and exposure-specific analysis. With the interaction term of age × sex, 45 and 95 DEGs were identified for 3 wk vs. 5 months and 3 wk vs. 10 months, respectively. Forty-three (96%) of 45 DEGs from 3 wk vs. 5 months and 89 (94%) of 95 DEGs from 3 wk vs. 10 months were also found in the sex- and exposure-specific analysis (Excel Table S8). No DEGs were found corresponding to any of the two interaction terms. We next conducted RNA-enrich pathway analysis to assess the gene pathways differentially expressed between weaning and 10 months of age in each group. Full lists of enriched GO pathways can be found in Excel Tables S9–S11. Figure 4C illustrates the number of significantly enriched GOBP pathways for each group, as well as the number of pathways overlapping multiple conditions. This analysis revealed little overlap in differentially expressed pathways across the different conditions. A single pathway (extracellular matrix organization) was significantly altered in all sexes and exposure groups, while Pb-exposed males and females had the largest number of overlapping pathways (11 pathways total). Two pathways (tissue remodeling and muscle contraction) were significantly differentially expressed in all exposed groups but not in control, and there was one pathway unique to both male and female control groups (protein kinase B signaling).

Concordant Differences in Gene Expression and DNA Methylation across the Life Course

We next examined the extent to which the observed differences in DNA methylation and gene expression across time in control and exposed animals occurred at the same genes. To this end, we identified all related DEGs occurring between any of the three time point comparisons (weaning vs. 5 months, 5 months vs. 10 months, and weaning vs. 10 months) and determined whether they also showed differential DNA methylation between weaning and 10 months of age. As shown in Figure 5A, several genes in each group showed concomitant differences in DNA methylation and gene expression. Full lists of these genes, as well as separate Venn diagrams for each of the three time point comparisons, can be found in Excel Table S12 and Figure S5. Notably, a subset of genes showed significant differential methylation and expression

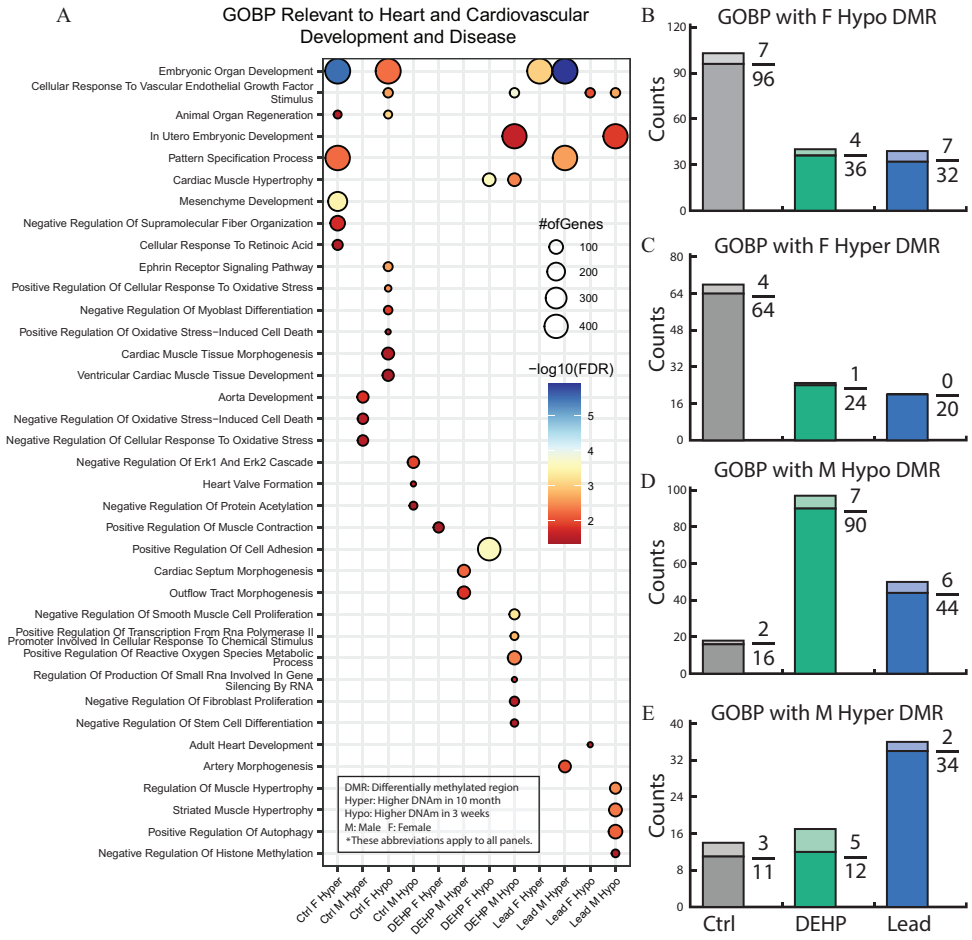

Figure 3. Pathway analysis of differences in DNA methylation between 3 wk and 10 months of age. (A) Summary of the significant Gene Ontology biological process (GOBP) terms for each combination of sex, exposure, and direction of methylation change, which are relevant to cardiovascular development and disease. The size of each circle reflects the number of genes in each category, and color indicates the −log10(FDR). (B–E) Number of enriched GOBP pathways for each combination of sex, exposure, and direction of methylation change. The numerator of each fraction depicts the number of pathways containing heart-related terms (muscle, ventricular, atrial cardiac, aorta, and heart), and the denominator depicts the number of all other pathways. The data for panel A can be found in Table S4. $n = 5$–7 mice per condition, as outlined in Figure 1. Note: Ctrl, control; DEHP, diethylhexyl phthalate; DMR, differentially methylated region; F, female; FDR, false discovery rate; M, male.

across time in exposed but not control hearts (25 and 20 genes in males and females, respectively). Several of these genes exhibited expression differences across time that differed by sex and exposure, including *Krt18* (found in DEHP male, Pb male, and Pb female), *Atp8a2* (found in DEHP- and Pb-exposed females), *Ston2* (found in DEHP- and Pb-exposed females, Pb male), and *Pou3f1* (found in DEHP- and Pb-exposed males) (Figure 5B–E).

Shifts in Cell Type across Life Stage in Mice Perinatally Exposed to Control, Pb, or DEHP

To examine whether observed differences in gene expression and DNA methylation were due to age- or exposure-related shifts in cellular composition, we conducted cell type deconvolution of the RNA-Seq data using a published algorithm and publicly available single-cell transcriptomic data[86,88] and quantified the relative proportions of atrial and ventricular cardiomyocytes, endothelial cells, smooth muscle cells, fibroblasts, adipocytes, lymphoid and myeloid cells, neuronal cells, pericytes, and mesothelial cells. Endothelial and smooth muscle cells were present in the largest proportions, followed by atrial and ventricular cardiomyocytes, while neuronal and mesothelial cells comprised the smallest proportions of cells (Figure S6). Summary statistics for all of the comparisons by age and exposure can be found in Excel Table S13. Overall, age-related trends in cell composition were generally consistent across sexes and exposure groups. The proportions of atrial cardiomyocytes remained consistent with age in all conditions (Figure S6A). Proportions of ventricular cardiomyocytes were higher at 10 months of age compared to weaning across all conditions ($p > 0.05$) (Figure S6B). However, in males exposed to Pb and DEHP, the higher proportion of ventricular cardiomyocytes was present at 5 months of age in contrast to controls which did not show differences until 10 months of age (Figure S6B). In mice from both sexes, there was a decline in the proportion of smooth muscle cells in control and DEHP-exposed mice across time ($p < 0.05$) but no change in Pb-exposed mice (Figure S6C). Temporal trends in the proportions of endothelial cells did not differ across exposure groups (Figure S6D). In control and exposed males, fibroblast proportions were significantly lower between weaning and 10 months of age ($p > 0.05$), a trend that was only present in Pb-exposed females (Figure S6E). The proportions of adipocytes across time were higher in all conditions ($p < 0.05$), with no differences by exposure (Figure S6F). Pericyte proportions were significantly higher with age in control males ($p < 0.05$), but this difference was not observed in exposed males or in females under any condition (Figure S6G). Proportions of neuronal cells did not significantly differ by time point, except in Pb-treated males and females ($p < 0.05$), where they were lower compared to baseline between weaning and 10 months of age

Table 2. Number of significantly differentially expressed genes (DEGs) between 3 weeks and 5 months of age, between 5 months and 10 months of age, and between 3 weeks and 10 months of age.

	3 weeks vs. 5 months		5 months vs. 10 months		3 weeks vs. 10 months	
Exposure	Male	Female	Male	Female	Male	Female
Control	461	825	48	569	421	933
DEHP	535	365	552	133	787	468
Pb	575	612	166	382	591	765

Note: Significance was based on an FDR < 0.05 and absolute log2(fold change) >2. $n = 5$–7 mice per condition, as outlined in Figure 1. DEHP, diethylhexyl phthalate; Pb, lead.

(Figure S6H). Lymphoid cell proportions trended up across time, a pattern that reached statistical significance in Pb-exposed females as well as control and DEHP-exposed males (Figure S6I). Myeloid cells were significantly higher at 10 months of age compared to weaning in all conditions except Pb-exposed females, which exhibited a trend toward significance (Figure S6J). No temporal differences in mesothelial cells were observed in any of the conditions (Figure S6K).

Discussion

Cardiac development begins in early embryogenesis, and growth and maturation continue during the postnatal period and adolescence.[90] Although development is largely complete by adolescence, the heart continues to undergo normal age-related changes in physiology, at a rate which varies based on the individual.[91] Cardiac development and aging are characterized by widespread transcriptional, epigenetic, and metabolic changes,[92–94] but how chemical exposures may interfere with these processes and the potential health effects are unknown. Studies showing widely divergent age-related epigenetic patterns in pairs of twins underscore the influence of environmental factors on the epigenome across time.[95–97] Such environmental deflection of the normal aging process, as we have previously defined it,[98] may have important implications for long-term disease risk.

In this study, we demonstrated that in controls and upon developmental exposure to two chemically distinct and ubiquitous environmental contaminants, marked differences in DNA methylation and expression of various gene pathways occurred between weaning and middle age in mice. In humans, development and aging are associated with altered DNA methylation at various stages across the life course, including in childhood,[95,99] between early childhood and adolescence,[100,101] and during adulthood and old age.[102,103] Temporal changes in DNA methylation have been characterized in numerous human tissues, including peripheral blood and various blood cell types, buccal epithelium, brain, kidney, skeletal muscle, prostate, liver, adipose, and cervix,[95,103–106] and similar profiling studies have been conducted in rodent tissues.[107–109] To our knowledge, no investigations into the effects of normal development and aging on DNA methylation and gene expression in the heart have been conducted in humans to date.

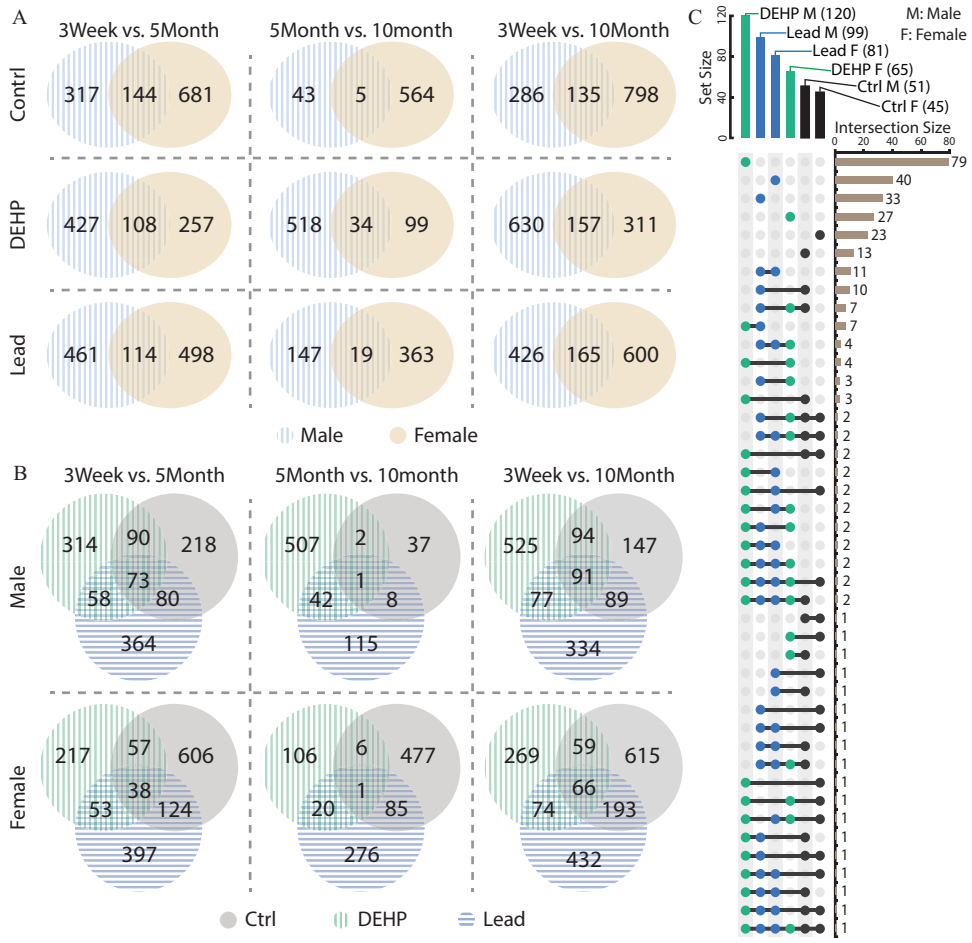

Figure 4. Sex and exposure specificity of transcriptomic differences between time points. (A) Venn diagrams showing sex overlap in differential gene expression for each time bracket comparison and exposure. (B) Venn diagram showing exposure overlap in differential gene expression for each time bracket comparison and sex. (C) UpSet plot showing the number of intersecting GOBP pathways for each exposure and sex combination. The data for this figure can be found in Excel Tables S5–S7, and S15. $n = 5$–7 mice per condition, as outlined in Figure 1. Note: Ctrl, control; DEHP, diethylhexyl phthalate.

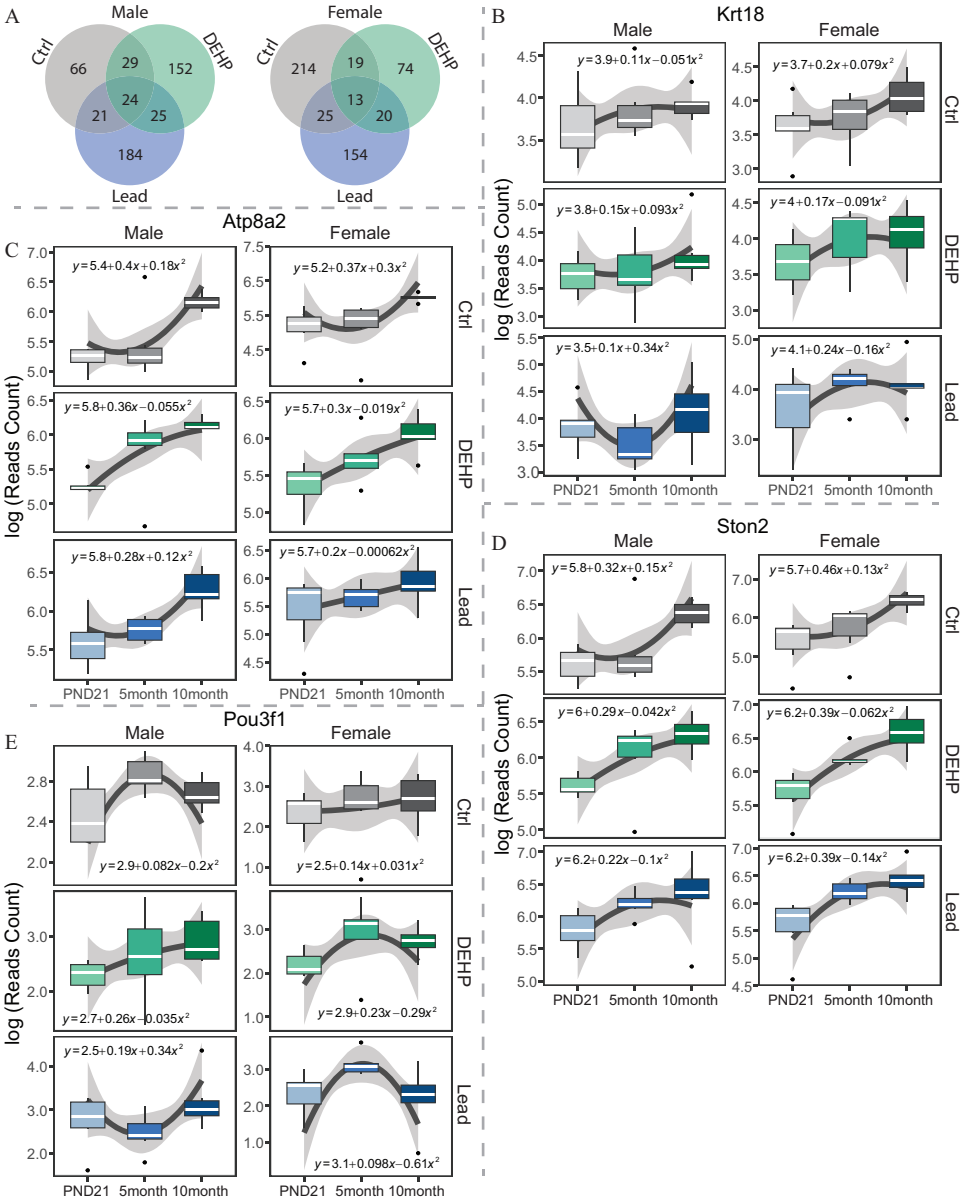

Figure 5. Genes with differential expression and DNA methylation. (A) Venn diagrams showing the number of genes in each sex exhibiting differential expression in any of the three time point comparisons (weaning vs. 5 months of age, 5 months of age vs. 10 months of age, and weaning vs. 10 months of age) and differential methylation. (B–E) RNA-Seq read count data for four genes showing that the age-related gene expression trajectory differs by exposure and/or sex. Each of the four genes were differentially expressed and methylated with one or both exposures but not in control. The boxplot shows the natural log-transformed read counts of each gene at each time point. Each of the boxplots represents five values: the median, the first quartile, the third quartile, and the two whiskers represent the largest or smallest values at most 1.5 times the interquartile range. The regression line is calculated using a generalized linear model in R (version 4.2.2; R Development Core Team). The data for panels B to E can be found in Table S14. $n = 5$–7 mice per condition, as outlined in Figure 1. Note: Ctrl, control; DEHP, diethylhexyl phthalate; PND, postnatal day.

Although one study did profile age-related changes in DNA methylation the mouse heart, females were not included.[108] This study is therefore impactful, as we examined how age affects the epigenome and gene expression in the heart in both males and females at baseline and in response to two toxicants of high relevance to humans.

Environmental Factors and Regulation of Gene Expression across the Life Course

Although studies in twins or nontwin family members[96,97,110] strongly suggest that environmental factors impact the aging process, the influence of specific chemicals on the epigenome across the life course is poorly understood. However, a number of recent studies have begun to shed light on this. In humans, these studies are largely restricted to blood, with few studies reporting effects on tissues targeted by the chemical exposures. Benzene, trichloroethylene, organochlorine pesticides, and PFAS, as well as air pollutants such as tobacco smoke, particulate matter, sulfate, and ammonium have all been associated with accelerated aging as measured via well-established DNA methylation clocks in blood.[111–115] Investigation of human liver samples showed that alcohol dependence is associated with increased DNA methylation age in the liver.[116] Animal studies have provided additional evidence that bisphenol A, Pb, and trichloroethylene can impact epigenetic aging of various tissues, through DNA methylation and

other epigenetic factors.[117–120] Mouse studies of Pb exposure and epigenetic aging to date have examined age-related DNA methylation of several loci in tail tissue[118] or expression of specific microRNAs (miRNAs) in the brain.[120] Few studies, however, have investigated how chemical exposures impact programming of the transcriptome and epigenome in the critical period between childhood and middle age. Moreover, little is known about how epigenetic regulation of gene expression in the heart changes across any stage of life. Our study thus addresses an important knowledge gap in this area.

Direction of DNA Methylation Differences across Time

In this study, we observed that the majority of age-related DMRs were hypermethylated, irrespective of age, sex, or exposure. This finding is in keeping with our previous work, which showed a general trend toward DNA hypermethylation in longitudinal mouse blood samples between 2 and 10 months of age.[121] In contrast, numerous studies demonstrate that aging is associated with genome-wide hypomethylation.[122–124] However, the period between weaning and 10 months of age analyzed in our study encompassed the early perinatal phase, puberty/adolescence, and adulthood. Effects of developmental exposure to these chemicals on old age will be an important area for future investigation. Previously published work in human blood has shown that global DNA methylation increases during early postnatal life, remains stable during adulthood, and then only declines with old age.[95,100,122,123] We also observed hypermethylation of CpG islands and promoters across the life course in both sexes and in all three exposure groups, in accordance with previous work.[122–124] Thus, our findings are consistent with temporal trends observed in other studies.

Differentially Expressed Genes and Associated Pathways in Mice Exposed to Pb and DEHP

We found that age-related DNA methylation occurred to a large extent in pathways related to tissue development and cell fate commitment. This aligns with work from others showing that age-related DNA methylation occurred at pathways related to development, obesity, longevity, and cancer across multiple species.[125] Although we observed differences in pathways related to development and differentiation across all conditions in general, the specific pathways enriched within each sex and exposure group were largely unique, suggesting that differences in cardiac DNA methylation across time exhibited sex specificity in unexposed animals, and were altered in distinct ways by developmental exposure to Pb or DEHP. Our transcriptional analysis revealed similar sex-specific differences in gene expression across the life course. Notably, pathway analysis of these data showed that Gene Ontology pathways related to tissue remodeling and muscle contraction were significantly altered between weaning and 10 months of age in males and females exposed to Pb or DEHP. As defects in both processes are implicated in a variety of CVDs,[126,127] it will be important to investigate the long-term effects of Pb exposure on cardiac function, an important future direction of this work.

Although the majority of age-related differential DNA methylation and gene expression did not occur in the same genes, we observed several genes that were both differentially methylated and expressed with age in each exposure group. Several genes, including *Atp8a2*, *Krt18*, *Pou3f1*, and *Ston2*, showed temporal gene expression differences that varied by sex and/or exposure. Although cardiovascular functions for *Atp8a2* and *Ston2* have not yet been reported, the *Krt18* gene was recently reported to play a protective role in heart failure in mice.[128] *Pou3f1* is a neurogenic factor that has been shown to be upregulated upon epigenetic dysregulation of normal cardiac differentiation of mouse embryonic stem cells.[129] Interrogation of the Comparative Toxicogenomics Database[80] revealed that all four genes are differentially expressed and/or methylated in response to numerous chemicals with diverse mechanisms of toxicity, including bisphenol A and benzo(a)pyrene, suggesting that these genes may represent biomarkers of chemical exposure. As we were statistically underpowered to detect quantitative changes in methylation and expression of individual genes, additional studies are needed to validate our findings.

Differences in Cellular Composition across Life Stage and Health Implications

The heart is comprised of several different cell types, including cardiomyocytes, fibroblasts, endothelial cells, pericytes, smooth muscle cells, adipocytes, immune cells, and neuronal and glial cells.[86] Shifts in cardiac cellularity across the life course have been reported, including increased fibrosis in old age[130] as well as changes in the composition of epicardial fat tissue,[131] but the effects of developmental exposures on changes in cellularity between weaning and middle adulthood are unknown. Age- and exposure-related epigenetic differences in whole tissue samples may be due to cell intrinsic changes, but they may also reflect alterations in cell type composition.[132] Because cellular composition of the heart is known to be influenced by age, disease, and sex,[130,131,133] we utilized cell type deconvolution to examine the extent to which the observed differences in DNA methylation and gene expression across time were due to altered cellular composition. We observed subtle but statistically significant differences in cell type proportions based on age, sex, and exposure. Thus, the differences in gene expression and DNA methylation over time observed in this study were likely due to both cell intrinsic transcriptional and epigenetic alterations, as well as alterations in cellular composition in the heart. Future studies using single-cell approaches will shed further light on this question.

The health implications of Pb- or DEHP-mediated changes in DNA methylation and gene expression in the heart are unclear, but several lines of evidence suggest that age-related changes in DNA methylation may impact long-term cardiovascular health. In mice, age-related DNA methylation is associated with more severe injury following an ischemia–reperfusion event.[134] Several human studies have also linked epigenetic age acceleration with an increased risk of various markers of cardiovascular disease in both white and black populations,[17,135–137] though sex differences and contributions of environmental factors are unclear.

Potential Molecular Mechanisms

The molecular mechanisms underlying age-related DNA methylation by Pb or DEHP exposure in control and exposed heart are currently unclear. Methylation of DNA is carried out by DNA methyltransferases (DNMT1, DNMT3A, DNMT3B), using *S*-adenosylmethionine (SAM) as a cofactor. DNA hydroxymethylation, the first step in the process of active DNA demethylation, is catalyzed by TET dioxygenases (TET1, TET2, TET3) with alpha ketoglutarate (α-KG), iron, and vitamin C as cofactors.[138] DNA methylation differences may thus result from altered expression or function of these enzymes or depletion of their cofactors. Studies in various cellular and animal models show that both DEHP and Pb can alter expression of DNMTs and/or TETs.[139–143] There is some evidence that both Pb and DEHP may alter levels of SAM, but there is otherwise little known about how these toxicants impact other cofactors for epigenetic modifying enzymes.[144,145] Pb and DEHP both have been shown to cause oxidative stress in multiple contexts[146,147] and given that DNA methylation is sensitive to cellular redox status,[148] this is another plausible mechanism of epigenetic programming by these chemicals. It is important to note that numerous other cellular targets are also sensitive to oxidative stress

and altered levels of cofactors such as SAM and α-KG.[149–151] Thus, the toxic effects of these chemicals may be independent of alterations to the epigenome altogether.

Study Limitations

This study has a few key limitations. First, these data represent a relatively small sample size in one mouse strain, and further experiments will be necessary to confirm our findings. In addition, to measure DNA methylation, we utilized a sodium bisulfite conversion-based method, which does not discriminate between 5-methylcytosine and other, more-oxidized modifications such as 5-hydroxymethylcytosine.[152] Thus, the differentially methylated cytosines and regions reported here reflect a combination of all of these modifications. Although 5-hydroxymethylcytosine is approximately an order of magnitude less abundant than 5-methylcytosine,[153] recent studies suggest that the modification has its own distinct molecular functions and plays an important role in cardiac development and disease.[154] Identifying age- and exposure-induced changes in 5-hydroxymethylcytosine is an important future direction of this research. Second, we examined DNA methylation differences using enhanced reduced representation bisulfite sequencing (ERRBS). Compared to classical reduced representation bisulfite sequencing (RRBS), which covers >70% of promoter regions and >75% of CG-rich regions, ERRBS improves coverage to >80% and >85%, respectively.[72] Despite this improved coverage, a limitation of ERRBS is that, compared to whole-genome bisulfite sequencing (WGBS), it covers GC-rich loci,[72] which, in our hands, encompassed ∼5% of the whole genome. Last, as the age–exposure and age–sex interaction terms were not significant in our models, we were statistically underpowered to detect quantitative changes in DNA methylation and expression of individual genes. Validation studies looking at transcript and protein expression of individual genes are therefore necessary to make more definitive conclusions about specific targets.

Conclusion

In summary, we demonstrated herein that developmental exposure to Pb or DEHP altered DNA methylation and expression of various pathways in the heart of mice in a sex-specific manner, long after cessation of exposure. Given that the risk of cardiovascular disease increases markedly with age, future studies should investigate how these differences may impact long-term cardiovascular health.

Acknowledgments

Funding for this work was provided by the National Institute of Environmental Health Sciences (NIEHS) TaRGET II Consortium U01 (ES026697), a NIEHS Transition to Independent Environmental Health Researcher (TIEHR) K01 (ES032048), a NIEHS Revolutionizing Innovative, Visionary Environmental Health Research (RIVER) R35 (ES031686), a National Institute of Aging R01 (AG072396), the University of Michigan NIEHS/EPA Children's Environmental Health and Disease Prevention Center P01 (ES022844/RD83543601), the Michigan Center on Lifestage Environmental Exposures and Disease (M-LEEaD), NIEHS T32 (ES007062), NIEHS R01 (ES028802), NIEHS grant K99 (ES034429), and the Michigan Biological Research Initiative on Sex Differences in Cardiovascular Disease (M-BRISC).

All sequencing data are available on the Sequencing Read Archive under ID number PRJNA1186815.

References

1. Thornburg KL. 2015. The programming of cardiovascular disease. J Dev Orig Health Dis 6(5):366–376, PMID: 26173733, https://doi.org/10.1017/S2040174415001300.
2. Powell-Wiley TM, Poirier P, Burke LE, Després J-P, Gordon-Larsen P, Lavie CJ, et al. 2021. Obesity and cardiovascular disease: a scientific statement from the American Heart Association. Circulation 143(21):e984–e1010, PMID: 33882682, https://doi.org/10.1161/CIR.0000000000000973.
3. Luscher TF. 2016. Prevention: some important steps forward, but many unmet needs in a world with cardiovascular disease as the leading cause of death. Eur Heart J 37(42):3179–3181, PMID: 27856560, https://doi.org/10.1093/eurheartj/ehw566.
4. Roth GA, Johnson C, Abajobir A, Abd-Allah F, Abera SF, Abyu G, et al. 2017. Global, regional, and national burden of cardiovascular diseases for 10 causes, 1990 to 2015. J Am Coll Cardiol 70(1):1–25, PMID: 28527533, https://doi.org/10.1016/j.jacc.2017.04.052.
5. Lam CSP, Arnott C, Beale AL, Chandramouli C, Hilfiker-Kleiner D, Kaye DM, et al. 2019. Sex differences in heart failure. Eur Heart J 40(47):3859–3868, PMID: 31800034, https://doi.org/10.1093/eurheartj/ehz835.
6. Ramirez LA, Sullivan JC. 2018. Sex differences in hypertension: where we have been and where we are going. Am J Hypertens 31(12):1247–1254, PMID: 30299518, https://doi.org/10.1093/ajh/hpy148.
7. Deegan DF, Nigam P, Engel N. 2021. Sexual dimorphism of the heart: genetics, epigenetics, and development. Front Cardiovasc Med 8:668252, PMID: 34124200, https://doi.org/10.3389/fcvm.2021.668252.
8. Cosselman KE, Navas-Acien A, Kaufman JD. 2015. Environmental factors in cardiovascular disease. Nat Rev Cardiol 12(11):627–642, PMID: 26461967, https://doi.org/10.1038/nrcardio.2015.152.
9. Pencina MJ, Navar AM, Wojdyla D, Sanchez RJ, Khan I, Elassal J, et al. 2019. Quantifying importance of major risk factors for coronary heart disease. Circulation 139(13):1603–1611, PMID: 30586759, https://doi.org/10.1161/CIRCULATIONAHA.117.031855.
10. Hamczyk MR, Nevado RM, Barettino A, Fuster V, Andres V. 2020. Biological versus chronological aging: JACC focus seminar. J Am Coll Cardiol 75(8):919–930, PMID: 32130928, https://doi.org/10.1016/j.jacc.2019.11.062.
11. Kankaanpaa A, Tolvanen A, Heikkinen A, Kaprio J, Ollikainen M, Sillanpaa E. 2022. The role of adolescent lifestyle habits in biological aging: a prospective twin study. eLife 11:e80729, PMID: 36345722, https://doi.org/10.7554/eLife.80729.
12. Enroth S, Enroth SB, Johansson A, Gyllensten U. 2015. Protein profiling reveals consequences of lifestyle choices on predicted biological aging. Sci Rep 5:17282, PMID: 26619799, https://doi.org/10.1038/srep17282.
13. Benedicto I, Dorado B, Andres V. 2021. Molecular and cellular mechanisms driving cardiovascular disease in Hutchinson-Gilford progeria syndrome: lessons learned from animal models. Cells 10(5):1157, PMID: 34064612, https://doi.org/10.3390/cells10051157.
14. Forrester SN, Zmora R, Schreiner PJ, Jacobs DR, Roger VL, Thorpe RJ, et al. 2021. Accelerated aging: a marker for social factors resulting in cardiovascular events? SSM Popul Health 13:100733, PMID: 33532540, https://doi.org/10.1016/j.ssmph.2021.100733.
15. Zhang D, Leeuwenburgh C, Zhou D, Gong Y, Pahor M, Licht JD, et al. 2022. Analysis of biological aging and risks of all-cause and cardiovascular disease-specific death in cancer survivors. JAMA Netw Open 5(6):e2218183, PMID: 35731518, https://doi.org/10.1001/jamanetworkopen.2022.18183.
16. Zhang W, Song M, Qu J, Liu GH. 2018. Epigenetic modifications in cardiovascular aging and diseases. Circ Res 123(7):773–786, PMID: 30355081, https://doi.org/10.1161/CIRCRESAHA.118.312497.
17. Joyce BT, Gao T, Zheng Y, Ma J, Hwang S-J, Liu L, et al. 2021. Epigenetic age acceleration reflects long-term cardiovascular health. Circ Res 129(8):770–781, PMID: 34428927, https://doi.org/10.1161/CIRCRESAHA.121.318965.
18. Liu D, Aziz NA, Pehlivan G, Breteler MMB. 2023. Cardiovascular correlates of epigenetic aging across the adult lifespan: a population-based study. Geroscience 45(3):1605–1618, PMID: 36752898, https://doi.org/10.1007/s11357-022-00714-0.
19. Hartman RJG, Huisman SE, den Ruijter HM. 2018. Sex differences in cardiovascular epigenetics—a systematic review. Biol Sex Differ 9(1):19, PMID: 29792221, https://doi.org/10.1186/s13293-018-0180-z.
20. Balali-Mood M, Naseri K, Tahergorabi Z, Khazdair MR, Sadeghi M. 2021. Toxic mechanisms of five heavy metals: mercury, lead, chromium, cadmium, and arsenic. Front Pharmacol 12:643972, PMID: 33927623, https://doi.org/10.3389/fphar.2021.643972.
21. Koch HM, Preuss R, Angerer J. 2006. Di(2-ethylhexyl)phthalate (DEHP): human metabolism and internal exposure– an update and latest results. Int J Androl 29(1):155–165, PMID: 16466535, https://doi.org/10.1111/j.1365-2605.2005.00607.x.
22. Obeng-Gyasi E. 2019. Sources of lead exposure in various countries. Rev Environ Health 34(1):25–34, PMID: 30854835, https://doi.org/10.1515/reveh-2018-0037.
23. Abadin H, Ashizawa A, Stevens YW, Llados F, Diamond G, Sage G, et al. 2007. *Toxicological Profile for Lead*. Atlanta, GA: Agency for Toxic Substances and Disease Registry.

24. Heudorf U, Mersch-Sundermann V, Angerer J. 2007. Phthalates: toxicology and exposure. Int J Hyg Environ Health 210(5):623–634, PMID: 17889607, https://doi.org/10.1016/j.ijheh.2007.07.011.
25. Engel SM, Patisaul HB, Brody C, Hauser R, Zota AR, Bennet DH, et al. 2021. Neurotoxicity of ortho-phthalates: recommendations for critical policy reforms to protect brain development in children. Am J Public Health 111(4):687–695, PMID: 33600256, https://doi.org/10.2105/AJPH.2020.306014.
26. Chen Z, Huo X, Chen G, Luo X, Xu X. 2021. Lead (Pb) exposure and heart failure risk. Environ Sci Pollut Res Int 28(23):28833–28847, PMID: 33840028, https://doi.org/10.1007/s11356-021-13725-9.
27. Menke A, Muntner P, Batuman V, Silbergeld EK, Guallar E. 2006. Blood lead below 0.48 micromol/L (10 microg/dL) and mortality among US adults. Circulation 114(13):1388–1394, PMID: 16982939, https://doi.org/10.1161/CIRCULATIONAHA.106.628321.
28. Kiełtucki J, Dobrakowski M, Pawlas N, Średniawa B, Boroń M, Kasperczyk S. 2017. The analysis of QT interval and repolarization morphology of the heart in chronic exposure to lead. Hum Exp Toxicol 36(10):1081–1086, PMID: 27903879, https://doi.org/10.1177/0960327116680277.
29. Navas-Acien A, Guallar E, Silbergeld EK, Rothenberg SJ. 2007. Lead exposure and cardiovascular disease–a systematic review. Environ Health Perspect 115(3):472–482, PMID: 17431501, https://doi.org/10.1289/ehp.9785.
30. Ou Y, Bloom MS, Nie Z, Han F, Mai J, Chen J, et al. 2017. Associations between toxic and essential trace elements in maternal blood and fetal congenital heart defects. Environ Int 106:127–134, PMID: 28645012, https://doi.org/10.1016/j.envint.2017.05.017.
31. Trasande L, Attina TM. 2015. Association of exposure to di-2-ethylhexylphthalate replacements with increased blood pressure in children and adolescents. Hypertension 66(2):301–308, PMID: 26156503, https://doi.org/10.1161/HYPERTENSIONAHA.115.05603.
32. Zeng G, Zhang Q, Wang X, Wu KH. 2022. Low-level plasticizer exposure and all-cause and cardiovascular disease mortality in the general population. Environ Health 21(1):32, PMID: 35264146, https://doi.org/10.1186/s12940-022-00841-3.
33. Lind PM, Lind L. 2011. Circulating levels of bisphenol a and phthalates are related to carotid atherosclerosis in the elderly. Atherosclerosis 218(1):207–213, PMID: 21621210, https://doi.org/10.1016/j.atherosclerosis.2011.05.001.
34. Olsen L, Lind L, Lind PM. 2012. Associations between circulating levels of bisphenol A and phthalate metabolites and coronary risk in the elderly. Ecotoxicol Environ Saf 80:179–83, PMID: 22421452, https://doi.org/10.1016/j.ecoenv.2012.02.023.
35. Chen C-W, Tang S-Y, Hwang J-S, Chan C-C, Hsu C-C, Lin C-Y, et al. 2021. Association between levels of urine Di-(2-ethylhexyl)phthalate metabolites and heart rate variability in young adults. Toxics 9(12):351, PMID: 34941785, https://doi.org/10.3390/toxics9120351.
36. Su TC, Hwang JJ, Sun CW, Wang SL. 2019. Urinary phthalate metabolites, coronary heart disease, and atherothrombotic markers. Ecotoxicol Environ Saf 173:37–44, PMID: 30753939, https://doi.org/10.1016/j.ecoenv.2019.02.021.
37. Pant N, Kumar G, Upadhyay AD, Patel DK, Gupta YK, Chaturvedi PK. 2014. Reproductive toxicity of lead, cadmium, and phthalate exposure in men. Environ Sci Pollut Res Int 21(18):11066–11074, PMID: 24816463, https://doi.org/10.1007/s11356-014-2986-5.
38. Govarts E, Remy S, Bruckers L, Den Hond E, Sioen I, Nelen V, et al. 2016. Combined effects of prenatal exposures to environmental chemicals on birth weight. Int J Environ Res Public Health 13(5):495, PMID: 27187434, https://doi.org/10.3390/ijerph13050495.
39. Papaioannou N, Distel E, de Oliveira E, Gabriel C, Frydas IS, Anesti O, et al. 2021. Multi-omics analysis reveals that co-exposure to phthalates and metals disturbs urea cycle and choline metabolism. Environ Res 192:110041, PMID: 32949613, https://doi.org/10.1016/j.envres.2020.110041.
40. Chi Z, Yang H, Liu J. 2024. Study on the combined toxicity of DEHP and lead on the blood system of rats. Chemosphere 349:140908, PMID: 38072204, https://doi.org/10.1016/j.chemosphere.2023.140908.
41. Perng W, Tamayo-Ortiz M, Tang L, Sánchez BN, Cantoral A, Meeker JD, et al. 2019. Early Life Exposure in Mexico to ENvironmental Toxicants (ELEMENT) Project. BMJ Open 9(8):e030427, PMID: 31455712, https://doi.org/10.1136/bmjopen-2019-030427.
42. Chen Z, Myers R, Wei T, Bind E, Kassim P, Wang G, et al. 2014. Placental transfer and concentrations of cadmium, mercury, lead, and selenium in mothers, newborns, and young children. J Expo Sci Environ Epidemiol 24(5):537–544, PMID: 24756102, https://doi.org/10.1038/jes.2014.26.
43. Martinez-Razo LD, Martinez-Ibarra A, Vazquez-Martinez ER, Cerbon M. 2021. The impact of Di-(2-ethylhexyl) phthalate and Mono(2-ethylhexyl) phthalate in placental development, function, and pathophysiology. Environ Int 146:106228, PMID: 33157377, https://doi.org/10.1016/j.envint.2020.106228.
44. Arbuckle TE, Fisher M, MacPherson S, Lang C, Provencher G, LeBlanc A, et al. 2016. Maternal and early life exposure to phthalates: the plastics and personal-care products use in pregnancy (P4) study. Sci Total Environ 551–552:344–356, PMID: 26878646, https://doi.org/10.1016/j.scitotenv.2016.02.022.
45. Rygiel CA, Goodrich JM, Solano-González M, Mercado-García A, Hu H, Téllez-Rojo MM, et al. 2021. Prenatal lead (Pb) exposure and peripheral blood DNA methylation (5mC) and hydroxymethylation (5hmC) in Mexican adolescents from the ELEMENT birth cohort. Environ Health Perspect 129(6):067002, PMID: 34152198, https://doi.org/10.1289/EHP8507.
46. Montrose L, Goodrich JM, Morishita M, Kochmanski J, Klaver Z, Cavalcante R, et al. 2020. Neonatal lead (Pb) exposure and DNA methylation profiles in dried bloodspots. Int J Environ Res Public Health 17(18):6775, PMID: 32957503, https://doi.org/10.3390/ijerph17186775.
47. Li M-H, Wang J-J, Feng Y-Q, Liu X, Yan Z-H, Zhang X-J, et al. 2023. H3K4me3 as a target of di(2-ethylhexyl) phthalate (DEHP) impairing primordial follicle assembly. Chemosphere 310:136811, PMID: 36220427, https://doi.org/10.1016/j.chemosphere.2022.136811.
48. Schneider JS, Anderson DW, Kidd SK, Sobolewski M, Cory-Slechta DA. 2016. Sex-dependent effects of lead and prenatal stress on post-translational histone modifications in frontal cortex and hippocampus in the early postnatal brain. Neurotoxicology 54:65–71, PMID: 27018513, https://doi.org/10.1016/j.neuro.2016.03.016.
49. Petroff RL, Cavalcante RG, Colacino JA, Goodrich JM, Jones TR, Lalancette C, et al. 2023. Developmental exposures to common environmental contaminants, DEHP and lead, alter adult brain and blood hydroxymethylation in mice. Front Cell Dev Biol 11:1198148, PMID: 37384255, https://doi.org/10.3389/fcell.2023.1198148.
50. Rattan S, Beers HK, Kannan A, Ramakrishnan A, Brehm E, Bagchi I, et al. 2019. Prenatal and ancestral exposure to di(2-ethylhexyl) phthalate alters gene expression and DNA methylation in mouse ovaries. Toxicol Appl Pharmacol 379:114629, PMID: 31211961, https://doi.org/10.1016/j.taap.2019.114629.
51. Svoboda LK, Wang K, Jones TR, Colacino JA, Sartor MA, Dolinoy DC. 2021. Sex-specific alterations in cardiac DNA methylation in adult mice by perinatal lead exposure. Int J Environ Res Public Health 18(2):577, PMID: 33445541, https://doi.org/10.3390/ijerph18020577.
52. Svoboda LK, Wang K, Cavalcante RG, Neier K, Colacino JA, Sartor MA, et al. 2020. Sex-specific programming of cardiac DNA methylation by developmental phthalate exposure. Epigenet Insights 13:2516865720939971, PMID: 32864567, https://doi.org/10.1177/2516865720939971.
53. Wang T, Pehrsson EC, Purushotham D, Li D, Zhuo X, Zhang B, et al. 2018. The NIEHS TaRGET II consortium and environmental epigenomics. Nat Biotechnol 36(3):225–227, PMID: 29509741, https://doi.org/10.1038/nbt.4099.
54. Svoboda LK, Wang K, Goodrich JM, Jones TR, Colacino JA, Peterson KE, et al. 2023. Perinatal lead exposure promotes sex-specific epigenetic programming of disease-relevant pathways in mouse heart. Toxics 11(1):85, PMID: 36668811, https://doi.org/10.3390/toxics11010085.
55. Waterland RA, Jirtle RL. 2003. Transposable elements: targets for early nutritional effects on epigenetic gene regulation. Mol Cell Biol 23(15):5293–5300, PMID: 12861015, https://doi.org/10.1128/MCB.23.15.5293-5300.2003.
56. Weinhouse C, Anderson OS, Bergin IL, Vandenbergh DJ, Gyekis JP, Dingman MA, et al. 2014. Dose-dependent incidence of hepatic tumors in adult mice following perinatal exposure to bisphenol A. Environ Health Perspect 122(5):485–491, PMID: 24487385, https://doi.org/10.1289/ehp.1307449.
57. Neier K, Cheatham D, Bedrosian LD, Dolinoy DC. 2019. Perinatal exposures to phthalates and phthalate mixtures result in sex-specific effects on body weight, organ weights and intracisternal A-particle (IAP) DNA methylation in weanling mice. J Dev Orig Health Dis 10(2):176–187, https://doi.org/10.1017/S2040174418000430.
58. Calafat AM, Brock JW, Silva MJ, Gray LE, Reidy JA, Barr DB, et al. 2006. Urinary and amniotic fluid levels of phthalate monoesters in rats after the oral administration of di(2-ethylhexyl) phthalate and di-n-butyl phthalate. Toxicology 217(1):22–30, PMID: 16171919, https://doi.org/10.1016/j.tox.2005.08.013.
59. Lorber M, Calafat AM. 2012. Dose reconstruction of di(2-ethylhexyl) phthalate using a simple pharmacokinetic model. Environ Health Perspect 120(12):1705–1710, PMID: 23010619, https://doi.org/10.1289/ehp.1205182.
60. Wittassek M, Angerer J. 2008. Phthalates: metabolism and exposure. Int J Androl 31(2):131–138, PMID: 18070048, https://doi.org/10.1111/j.1365-2605.2007.00837.x.
61. Wittassek M, Angerer J, Kolossa-Gehring M, Schäfer SD, Klockenbusch W, Dobler L, et al. 2009. Fetal exposure to phthalates–a pilot study. Int J Hyg Environ Health 212(5):492–498, PMID: 19423389, https://doi.org/10.1016/j.ijheh.2009.04.001.
62. Silva MJ, Reidy JA, Herbert AR, Preau JL Jr, Needham LL, Calafat AM. 2004. Detection of phthalate metabolites in human amniotic fluid. Bull Environ Contam Toxicol 72(6):1226–1231, PMID: 15362453, https://doi.org/10.1007/s00128-004-0374-4.
63. Huang PC, Kuo PL, Chou YY, Lin SJ, Lee CC. 2009. Association between prenatal exposure to phthalates and the health of newborns. Environ Int 35(1):14–20, PMID: 18640725, https://doi.org/10.1016/j.envint.2008.05.012.
64. Kavlock R, Barr D, Boekelheide K, Breslin W, Breysse P, Chapin R, et al. 2006. NTP-CERHR expert panel update on the reproductive and developmental toxicity of di(2-ethylhexyl) phthalate. Reprod Toxicol 22(3):291–399, PMID: 17068859, https://doi.org/10.1016/j.reprotox.2006.04.007.
65. Lyche JL, Gutleb AC, Bergman A, Eriksen GS, Murk AJ, Ropstad E, et al. 2009. Reproductive and developmental toxicity of phthalates. J Toxicol Environ

Health B Crit Rev 12(4):225–249, PMID: 20183522, https://doi.org/10.1080/10937400903094091.
66. Faulk C, Barks A, Liu K, Goodrich JM, Dolinoy DC. 2013. Early-life lead exposure results in dose- and sex-specific effects on weight and epigenetic gene regulation in weanling mice. Epigenomics 5(5):487–500, PMID: 24059796, https://doi.org/10.2217/epi.13.49.
67. McFarland MJ, Hauer ME, Reuben A. 2022. Half of US population exposed to adverse lead levels in early childhood. Proc Natl Acad Sci USA 119(11): e2118631119, PMID: 35254913, https://doi.org/10.1073/pnas.2118631119.
68. Huo X, Peng L, Xu X, Zheng L, Qiu B, Qi Z, et al. 2007. Elevated blood lead levels of children in Guiyu, an electronic waste recycling town in China. Environ Health Perspect 115(7):1113–1117, PMID: 17637931, https://doi.org/10.1289/ehp.9697.
69. Caravanos J, Dowling R, Téllez-Rojo MM, Cantoral A, Kobrosly R, Estrada D, et al. 2014. Blood lead levels in Mexico and pediatric burden of disease implications. Ann Glob Health 80(4):269–277, PMID: 25459328, https://doi.org/10.1016/j.aogh.2014.08.002.
70. Dutta S, Sengupta P. 2016. Men and mice: relating their ages. Life Sci 152:244–248, PMID: 26596563, https://doi.org/10.1016/j.lfs.2015.10.025.
71. Svoboda LK, Neier K, Wang K, Cavalcante RG, Rygiel CA, Tsai Z, et al. 2021. Tissue and sex-specific programming of DNA methylation by perinatal lead exposure: implications for environmental epigenetics studies. Epigenetics 16(10):1102–1122, PMID: 33164632, https://doi.org/10.1080/15592294.2020.1841872.
72. Garrett-Bakelman FE, Sheridan CK, Kacmarczyk TJ, Ishii J, Betel D, Alonso A, et al. 2015. Enhanced reduced representation bisulfite sequencing for assessment of DNA methylation at base pair resolution. J Vis Exp (96):e52246, PMID: 25742437, https://doi.org/10.3791/52246.
73. Krueger F, Andrews SR. 2011. Bismark: a flexible aligner and methylation caller for bisulfite-seq applications. Bioinformatics 27(11):1571–1572, PMID: 21493656, https://doi.org/10.1093/bioinformatics/btr167.
74. Langmead B, Salzberg SL. 2012. Fast gapped-read alignment with Bowtie 2. Nat Methods 9(4):357–359, PMID: 22388286, https://doi.org/10.1038/nmeth.1923.
75. Dobin A, Davis CA, Schlesinger F, Drenkow J, Zaleski C, Jha S, et al. 2013. STAR: ultrafast universal RNA-seq aligner. Bioinformatics 29(1):15–21, PMID: 23104886, https://doi.org/10.1093/bioinformatics/bts635.
76. Anders S, Pyl PT, Huber W. 2015. HTSeq–a Python framework to work with high-throughput sequencing data. Bioinformatics 31(2):166–169, PMID: 25260700, https://doi.org/10.1093/bioinformatics/btu638.
77. Risso D, Ngai J, Speed TP, Dudoit S. 2014. Normalization of RNA-seq data using factor analysis of control genes or samples. Nat Biotechnol 32(9):896–902, PMID: 25150836, https://doi.org/10.1038/nbt.2931.
78. Robinson MD, McCarthy DJ, Smyth GK. 2010. edgeR: a Bioconductor package for differential expression analysis of digital gene expression data. Bioinformatics 26(1):139–140, PMID: 19910308, https://doi.org/10.1093/bioinformatics/btp616.
79. Ritchie ME, Phipson B, Wu D, Hu Y, Law CW, Shi W, et al. 2015. Limma powers differential expression analyses for RNA-sequencing and microarray studies. Nucleic Acids Res 43(7):e47, PMID: 25605792, https://doi.org/10.1093/nar/gkv007.
80. Davis AP, Grondin CJ, Johnson RJ, Sciaky D, Wiegers J, Wiegers TC, et al. 2021. Comparative toxicogenomics database (CTD): update 2021. Nucleic Acids Res 49(D1):D1138–D1143, PMID: 33068428, https://doi.org/10.1093/nar/gkaa891.
81. Park Y, Figueroa ME, Rozek LS, Sartor MA. 2014. MethylSig: a whole genome DNA methylation analysis pipeline. Bioinformatics 30(17):2414–2422, PMID: 24836530, https://doi.org/10.1093/bioinformatics/btu339.
82. Cavalcante RG, Sartor MA. 2017. Annotatr: genomic regions in context. Bioinformatics 33(15):2381–2383, PMID: 28369316, https://doi.org/10.1093/bioinformatics/btx183.
83. Morgan M. 2024. AnnotationHub: Client to Access AnnotationHub Resources. https://bioconductor.org/packages/AnnotationHub [accessed 3 February 2024].
84. Yu G, Wang LG, Han Y, He QY. 2012. clusterProfiler: an R package for comparing biological themes among gene clusters. OMICS 16(5):284–287, PMID: 22455463, https://doi.org/10.1089/omi.2011.0118.
85. Welch RP, Lee C, Imbriano PM, Patil S, Weymouth TE, Smith RA, et al. 2014. ChIP-enrich: gene set enrichment testing for ChIP-seq data. Nucleic Acids Res 42(13):e105, PMID: 24878920, https://doi.org/10.1093/nar/gku463.
86. Litviňuková M, Talavera-López C, Maatz H, Reichart D, Worth CL, Lindberg EL, et al. 2020. Cells of the adult human heart. Nature 588(7838):466–472, PMID: 32971526, https://doi.org/10.1038/s41586-020-2797-4.
87. Hao Y, Hao S, Andersen-Nissen E, Mauck WM, Zheng S, Butler A, et al. 2021. Integrated analysis of multimodal single-cell data. Cell 184(13):3573–3587, PMID: 34062119, https://doi.org/10.1016/j.cell.2021.04.048.
88. Wang X, Park J, Susztak K, Zhang NR, Li M. 2019. Bulk tissue cell type deconvolution with multi-subject single-cell expression reference. Nat Commun 10(1):380, PMID: 30670690, https://doi.org/10.1038/s41467-018-08023-x.
89. Smedley D, Haider S, Ballester B, Holland R, London D, Thorisson G, et al. 2009. BioMart–biological queries made easy. BMC Genomics 10:22, PMID: 19144180, https://doi.org/10.1186/1471-2164-10-22.
90. Yang X, Pabon L, Murry CE. 2014. Engineering adolescence: maturation of human pluripotent stem cell-derived cardiomyocytes. Circ Res 114(3):511–523, PMID: 24481842, https://doi.org/10.1161/CIRCRESAHA.114.300558.
91. Cheitlin MD. 2003. Cardiovascular physiology—changes with aging. Am J Geriatr Cardiol 12(1):9–13, PMID: 12502909, https://doi.org/10.1111/j.1076-7460.2003.01751.x.
92. DeLaughter DM, Bick AG, Wakimoto H, McKean D, Gorham JM, Kathiriya IS, et al. 2016. Single-cell resolution of temporal gene expression during heart development. Dev Cell 39(4):480–490, PMID: 27840107, https://doi.org/10.1016/j.devcel.2016.10.001.
93. Gu Y, Zhou Y, Ju S, Liu X, Zhang Z, Guo J, et al. 2022. Multi-omics profiling visualizes dynamics of cardiac development and functions. Cell Rep 41(13):111891, PMID: 36577384, https://doi.org/10.1016/j.celrep.2022.111891.
94. Chen Y, Bravo JI, Son JM, Lee C, Benayoun BA. 2020. Remodeling of the H3 nucleosomal landscape during mouse aging. Transl Med Aging 4:22–31, PMID: 32462102, https://doi.org/10.1016/j.tma.2019.12.003.
95. Martino D, Loke YJ, Gordon L, Ollikainen M, Cruickshank MN, Saffery R, et al. 2013. Longitudinal, genome-scale analysis of DNA methylation in twins from birth to 18 months of age reveals rapid epigenetic change in early life and pair-specific effects of discordance. Genome Biol 14(5):R42, PMID: 23697701, https://doi.org/10.1186/gb-2013-14-5-r42.
96. Wang Y, Karlsson R, Lampa E, Zhang Q, Hedman ÅK, Almgren M, et al. 2018. Epigenetic influences on aging: a longitudinal genome-wide methylation study in old Swedish twins. Epigenetics 13(9):975–987, PMID: 30264654, https://doi.org/10.1080/15592294.2018.1526028.
97. Reynolds CA, Tan Q, Munoz E, Jylhävä J, Hjelmborg J, Christiansen L, et al. 2020. A decade of epigenetic change in aging twins: genetic and environmental contributions to longitudinal DNA methylation. Aging Cell 19(8):e13197, PMID: 32710526, https://doi.org/10.1111/acel.13197.
98. Kochmanski J, Montrose L, Goodrich JM, Dolinoy DC. 2017. Environmental deflection: the impact of toxicant exposures on the aging epigenome. Toxicol Sci 156(2):325–335, PMID: 28087834, https://doi.org/10.1093/toxsci/kfx005.
99. Urdinguio RG, Torró MI, Bayón GF, Álvarez-Pitti J, Fernández AF, Redon P, et al. 2016. Longitudinal study of DNA methylation during the first 5 years of life. J Transl Med 14(1):160, PMID: 27259700, https://doi.org/10.1186/s12967-016-0913-x.
100. Alisch RS, Barwick BG, Chopra P, Myrick LK, Satten GA, Conneely KN, et al. 2012. Age-associated DNA methylation in pediatric populations. Genome Res 22(4):623–632, PMID: 22300631, https://doi.org/10.1101/gr.125187.111.
101. Mulder RH, Neumann A, Cecil CAM, Walton E, Houtepen LC, Simpkin AJ, et al. 2021. Epigenome-wide change and variation in DNA methylation in childhood: trajectories from birth to late adolescence. Hum Mol Genet 30(1):119–134, PMID: 33450751, https://doi.org/10.1093/hmg/ddaa280.
102. Fraga MF, Ballestar E, Paz MF, Ropero S, Setien F, Ballestar ML, et al. 2005. Epigenetic differences arise during the lifetime of monozygotic twins. Proc Natl Acad Sci USA 102(30):10604–10609, PMID: 16009939, https://doi.org/10.1073/pnas.0500398102.
103. Day K, Waite LL, Thalacker-Mercer A, West A, Bamman MM, Brooks JD, et al. 2013. Differential DNA methylation with age displays both common and dynamic features across human tissues that are influenced by CpG landscape. Genome Biol 14(9):R102, PMID: 24034465, https://doi.org/10.1186/gb-2013-14-9-r102.
104. Bysani M, Perfilyev A, de Mello VD, Rönn T, Nilsson E, Pihlajamäki J, et al. 2017. Epigenetic alterations in blood mirror age-associated DNA methylation and gene expression changes in human liver. Epigenomics 9(2):105–122, PMID: 27911095, https://doi.org/10.2217/epi-2016-0087.
105. Kwabi-Addo B, Chung W, Shen L, Ittmann M, Wheeler T, Jelinek J, et al. 2007. Age-related DNA methylation changes in normal human prostate tissues. Clin Cancer Res 13(13):3796–3802, PMID: 17606710, https://doi.org/10.1158/1078-0432.CCR-07-0085.
106. Slieker RC, Relton CL, Gaunt TR, Slagboom PE, Heijmans BT. 2018. Age-related DNA methylation changes are tissue-specific with ELOVL2 promoter methylation as exception. Epigenetics Chromatin 11(1):25, PMID: 29848354, https://doi.org/10.1186/s13072-018-0191-3.
107. Thompson RF, Atzmon G, Gheorghe C, Liang HQ, Lowes C, Greally JM, et al. 2010. Tissue-specific dysregulation of DNA methylation in aging. Aging Cell 9(4):506–518, PMID: 20497131, https://doi.org/10.1111/j.1474-9726.2010.00577.x.
108. Stubbs TM, Bonder MJ, Stark A-K, Krueger F, von Meyenn F, Stegle O, et al. 2017. Multi-tissue DNA methylation age predictor in mouse. Genome Biol 18(1):68, PMID: 28399939, https://doi.org/10.1186/s13059-017-1203-5.
109. Maegawa S, Hinkal G, Kim HS, Shen L, Zhang L, Zhang J, et al. 2010. Widespread and tissue specific age-related DNA methylation changes in mice. Genome Res 20(3):332–340, PMID: 20107151, https://doi.org/10.1101/gr.096826.109.
110. Li S, Nguyen TL, Wong EM, Dugué P-A, Dite GS, Armstrong NJ, et al. 2020. Genetic and environmental causes of variation in epigenetic aging across the lifespan. Clin Epigenetics 12(1):158, PMID: 33092643, https://doi.org/10.1186/s13148-020-00950-1.
111. van der Laan L, Cardenas A, Vermeulen R, Fadadu RP, Hubbard AE, Phillips RV, et al. 2022. Epigenetic aging biomarkers and occupational exposure to

benzene, trichloroethylene and formaldehyde. Environ Int 158:106871, PMID: 34560324, https://doi.org/10.1016/j.envint.2021.106871.
112. de Prado-Bert P, Ruiz-Arenas C, Vives-Usano M, Andrusaityte S, Cadiou S, Carracedo Á, et al. 2021. The early-life exposome and epigenetic age acceleration in children. Environ Int 155:106683, PMID: 34144479, https://doi.org/10.1016/j.envint.2021.106683.
113. Nwanaji-Enwerem JC, Dai L, Colicino E, Oulhote Y, Di Q, Kloog I, et al. 2017. Associations between long-term exposure to PM(2.5) component species and blood DNA methylation age in the elderly: the VA normative aging study. Environ Int 102:57–65, PMID: 28284819, https://doi.org/10.1016/j.envint.2016.12.024.
114. Lind PM, Salihovic S, Lind L. 2018. High plasma organochlorine pesticide levels are related to increased biological age as calculated by DNA methylation analysis. Environ Int 113:109–113, PMID: 29421399, https://doi.org/10.1016/j.envint.2018.01.019.
115. Goodrich JM, Calkins MM, Caban-Martinez AJ, Stueckle T, Grant C, Calafat AM, et al. 2021. Per- and polyfluoroalkyl substances, epigenetic age and DNA methylation: a cross-sectional study of firefighters. Epigenomics 13(20):1619–1636, PMID: 34670402, https://doi.org/10.2217/epi-2021-0225.
116. Rosen AD, Robertson KD, Hlady RA, Muench C, Lee J, Philibert R, et al. 2018. DNA methylation age is accelerated in alcohol dependence. Transl Psychiatry 8(1):182, PMID: 30185790, https://doi.org/10.1038/s41398-018-0233-4.
117. Treviño LS, Dong J, Kaushal A, Katz TA, Jangid RK, Robertson MJ, et al. 2020. Epigenome environment interactions accelerate epigenomic aging and unlock metabolically restricted epigenetic reprogramming in adulthood. Nat Commun 11(1):2316, PMID: 32385268, https://doi.org/10.1038/s41467-020-15847-z.
118. Faulk C, Liu K, Barks A, Goodrich JM, Dolinoy DC. 2014. Longitudinal epigenetic drift in mice perinatally exposed to lead. Epigenetics 9(7):934–941, PMID: 24786859, https://doi.org/10.4161/epi.29024.
119. Gilbert KM, Blossom SJ, Erickson SW, Reisfeld B, Zurlinden TJ, Broadfoot B, et al. 2016. Chronic exposure to water pollutant trichloroethylene increased epigenetic drift in CD4(+) T cells. Epigenomics 8(5):633–649, PMID: 27092578, https://doi.org/10.2217/epi-2015-0018.
120. Wang R, Wu Z, Liu R, Bai L, Lin Y, Ba Y, et al. 2022. Age-related miRNAs dysregulation and abnormal BACE1 expression following Pb exposure in adolescent mice. Environ Toxicol 37(8):1902–1913, PMID: 35426476, https://doi.org/10.1002/tox.23536.
121. Kochmanski J, Marchlewicz EH, Cavalcante RG, Sartor MA, Dolinoy DC. 2018. Age-related epigenome-wide DNA methylation and hydroxymethylation in longitudinal mouse blood. Epigenetics 13(7):779–792, PMID: 30079798, https://doi.org/10.1080/15592294.2018.1507198.
122. Jones MJ, Goodman SJ, Kobor MS. 2015. DNA methylation and healthy human aging. Aging Cell 14(6):924–932, PMID: 25913071, https://doi.org/10.1111/acel.12349.
123. Heyn H, Li N, Ferreira HJ, Moran S, Pisano DG, Gomez A, et al. 2012. Distinct DNA methylomes of newborns and centenarians. Proc Natl Acad Sci USA 109(26):10522–10527, PMID: 22689993, https://doi.org/10.1073/pnas.1120658109.
124. Rakyan VK, Down TA, Maslau S, Andrew T, Yang T-P, Beyan H, et al. 2010. Human aging-associated DNA hypermethylation occurs preferentially at bivalent chromatin domains. Genome Res 20(4):434–439, PMID: 20219945, https://doi.org/10.1101/gr.103101.109.
125. Lu AT, Fei Z, Haghani A, Robeck TR, Zoller JA, Li CZ, et al. 2023. Universal DNA methylation age across mammalian tissues. Nat Aging 3(9):1144–1166, PMID: 37563227, https://doi.org/10.1038/s43587-023-00462-6.
126. Kuppe C, Ramirez Flores RO, Li Z, Hayat S, Levinson RT, Liao X, et al. 2022. Spatial multi-omic map of human myocardial infarction. Nature 608(7924):766–777, PMID: 35948637, https://doi.org/10.1038/s41586-022-05060-x.
127. Ren Z, Yu P, Li D, Li Z, Liao Y, Wang Y, et al. 2020. Single-cell reconstruction of progression trajectory reveals intervention principles in pathological cardiac hypertrophy. Circulation 141(21):1704–1719, PMID: 32098504, https://doi.org/10.1161/CIRCULATIONAHA.119.043053.
128. Papathanasiou S, Rickelt S, Soriano ME, Schips TG, Maier HJ, Davos CH, et al. 2015. Tumor necrosis factor-alpha confers cardioprotection through ectopic expression of keratins K8 and K18. Nat Med 21(9):1076–1084, PMID: 26280121, https://doi.org/10.1038/nm.3925.
129. Hota SK, Rao KS, Blair AP, Khalilimeybodi A, Hu KM, Thomas R, et al. 2022. Brahma safeguards canalization of cardiac mesoderm differentiation. Nature 602(7895):129–134, PMID: 35082446, https://doi.org/10.1038/s41586-021-04336-y.
130. Biernacka A, Frangogiannis NG. 2011. Aging and cardiac fibrosis. Aging Dis 2(2):158–173, PMID: 21837283.
131. Iacobellis G. 2021. Aging effects on epicardial adipose tissue. Front Aging 2:666260, PMID: 35822028, https://doi.org/10.3389/fragi.2021.666260.
132. Campbell KA, Colacino JA, Park SK, Bakulski KM. 2020. Cell types in environmental epigenetic studies: biological and epidemiological frameworks. Curr Environ Health Rep 7(3):185–197, PMID: 32794033, https://doi.org/10.1007/s40572-020-00287-0.
133. Lim GB. 2020. Complexity and plasticity of cardiac cellular composition. Nat Rev Cardiol 17(12):759, PMID: 33024278, https://doi.org/10.1038/s41569-020-00464-6.
134. Boovarahan SR, Ali N, AlAsmari AF, Alameen AA, Khan R, Kurian GA. 2022. Age-associated global DNA hypermethylation augments the sensitivity of hearts towards ischemia-reperfusion injury. Front Genet 13:995887, PMID: 36457746, https://doi.org/10.3389/fgene.2022.995887.
135. Roetker NS, Pankow JS, Bressler J, Morrison AC, Boerwinkle E. 2018. Prospective study of epigenetic age acceleration and incidence of cardiovascular disease outcomes in the ARIC study (atherosclerosis risk in communities). Circ Genom Precis Med 11(3):e001937, PMID: 29555670, https://doi.org/10.1161/CIRCGEN.117.001937.
136. Topriceanu C-C, Dev E, Ahmad M, Hughes R, Shiwani H, Webber M, et al. 2023. Accelerated DNA methylation age plays a role in the impact of cardiovascular risk factors on the human heart. Clin Epigenetics 15(1):164, PMID: 37853450, https://doi.org/10.1186/s13148-023-01576-9.
137. Wang C, Ni W, Yao Y, Just A, Heiss J, Wei Y, et al. 2021. DNA methylation-based biomarkers of age acceleration and all-cause death, myocardial infarction, stroke, and cancer in two cohorts: the NAS, and KORA F4. EBioMedicine 63:103151, PMID: 33279859, https://doi.org/10.1016/j.ebiom.2020.103151.
138. Wu SC, Zhang Y. 2010. Active DNA demethylation: many roads lead to Rome. Nat Rev Mol Cell Biol 11(9):607–620, PMID: 20683471, https://doi.org/10.1038/nrm2950.
139. Ghosh K, Chatterjee B, Nalla K, Behera B, Mukherjee A, Kanade SR. 2022. Di-(2-ethylhexyl) phthalate triggers DNA methyltransferase 1 expression resulting in elevated CpG-methylation and enrichment of MECP2 in the p21 promoter in vitro. Chemosphere 293:133569, PMID: 35033518, https://doi.org/10.1016/j.chemosphere.2022.133569.
140. Wen Y, Rattan S, Flaws JA, Irudayaraj J. 2020. Multi and transgenerational epigenetic effects of di-(2-ethylhexyl) phthalate (DEHP) in liver. Toxicol Appl Pharmacol 402:115123, PMID: 32628958, https://doi.org/10.1016/j.taap.2020.115123.
141. Sanchez OF, Lee J, Yu King Hing N, Kim SE, Freeman JL, Yuan C. 2017. Lead (Pb) exposure reduces global DNA methylation level by non-competitive inhibition and alteration of dnmt expression. Metallomics 9(2):149–160, PMID: 27934997, https://doi.org/10.1039/c6mt00198j.
142. Bihaqi SW, Huang H, Wu J, Zawia NH. 2011. Infant exposure to lead (Pb) and epigenetic modifications in the aging primate brain: implications for Alzheimer's disease. J Alzheimers Dis 27(4):819–33, PMID: 21891863, https://doi.org/10.3233/JAD-2011-111013.
143. Schneider JS, Kidd SK, Anderson DW. 2013. Influence of developmental lead exposure on expression of DNA methyltransferases and methyl cytosine-binding proteins in hippocampus. Toxicol Lett 217(1):75–81, PMID: 23246732, https://doi.org/10.1016/j.toxlet.2012.12.004.
144. Cao XJ, Huang SH, Wang M, Chen JT, Ruan DY. 2008. S-adenosyl-L-methionine improves impaired hippocampal long-term potentiation and water maze performance induced by developmental lead exposure in rats. Eur J Pharmacol 595(1–3):30–34, PMID: 18713624, https://doi.org/10.1016/j.ejphar.2008.07.061.
145. Li G, Zhao C-Y, Wu Q, Guan S-Y, Jin H-W, Na X-L, et al. 2021. Integrated metabolomics and transcriptomics reveal di(2-ethylhexyl) phthalate-induced mitochondrial dysfunction and glucose metabolism disorder through oxidative stress in rat liver. Ecotoxicol Environ Saf 228:112988, PMID: 34808505, https://doi.org/10.1016/j.ecoenv.2021.112988.
146. Paithankar JG, Saini S, Dwivedi S, Sharma A, Chowdhuri DK. 2021. Heavy metal associated health hazards: an interplay of oxidative stress and signal transduction. Chemosphere 262:128350, PMID: 33182141, https://doi.org/10.1016/j.chemosphere.2020.128350.
147. Wen ZJ, Wang ZY, Zhang YF. 2022. Adverse cardiovascular effects and potential molecular mechanisms of DEHP and its metabolites-a review. Sci Total Environ 847:157443, PMID: 35868369, https://doi.org/10.1016/j.scitotenv.2022.157443.
148. Domann FE, Hitchler MJ. 2021. Aberrant redox biology and epigenetic reprogramming: co-conspirators across multiple human diseases. Free Radic Biol Med 170:2–5, PMID: 33932538, https://doi.org/10.1016/j.freeradbiomed.2021.04.020.
149. Peoples JN, Saraf A, Ghazal N, Pham TT, Kwong JQ. 2019. Mitochondrial dysfunction and oxidative stress in heart disease. Exp Mol Med 51(12):1–13, PMID: 31857574, https://doi.org/10.1038/s12276-019-0355-7.
150. Liu S, He L, Yao K. 2018. The antioxidative function of alpha-ketoglutarate and its applications. Biomed Res Int 2018:3408467, PMID: 29750149, https://doi.org/10.1155/2018/3408467.
151. Martinez E, Gérard N, Garcia MM, Mazur A, Guéant-Rodriguez R-M, Comte B, et al. 2013. Myocardium proteome remodelling after nutritional deprivation of methyl donors. J Nutr Biochem 24(7):1241–1250, PMID: 23318136, https://doi.org/10.1016/j.jnutbio.2012.09.008.
152. Huang Y, Pastor WA, Shen Y, Tahiliani M, Liu DR, Rao A. 2010. The behaviour of 5-hydroxymethylcytosine in bisulfite sequencing. PLoS One 5(1):e8888, PMID: 20126651, https://doi.org/10.1371/journal.pone.0008888.
153. Yu M, Hon GC, Szulwach KE, Song C-X, Zhang L, Kim A, et al. 2012. Base-resolution analysis of 5-hydroxymethylcytosine in the mammalian genome. Cell 149(6):1368–1380, PMID: 22608086, https://doi.org/10.1016/j.cell.2012.04.027.
154. Greco CM, Kunderfranco P, Rubino M, Larcher V, Carullo P, Anselmo A, et al. 2016. DNA hydroxymethylation controls cardiomyocyte gene expression in development and hypertrophy. Nat Commun 7:12418, PMID: 27489048, https://doi.org/10.1038/ncomms12418.